Biosensors and Bioelectronics 194 (2021) 113609

Contents lists available at ScienceDirect

Biosensors and Bioelectronics

journal homepage: www.elsevier.com/locate/bios

Recent progress of self-powered respiration monitoring systems

Jieyu Dai [a,b], Linlin Li [a,b], Bojing Shi [c,*], Zhou Li [a,b,**]

[a] College of Chemistry and Chemical Engineering, Center on Nanoenergy Research, Guangxi University, 530004, Nanning, China
[b] Beijing Institute of Nanoenergy and Nanosystems, Chinese Academy of Sciences, 101400, Beijing, China
[c] Beijing Advanced Innovation Centre for Biomedical Engineering, Key Laboratory for Biomechanics and Mechanobiology of Ministry of Education, School of Biological Science and Medical Engineering, Beihang University, Beijing, 100191, China

ARTICLE INFO

Keywords:
Self-powered
Respiration sensor
Monitoring system
Wearable/implantable
Nanogenerator

ABSTRACT

Wearable and implantable medical devices are playing more and more key roles in disease diagnosis and health management. Various biosensors and systems have been used for respiration monitoring. Among them, self-powered sensors have some special characteristics such as low-cost, easy preparation, highly designable, and diversified. The respiratory airflow can drive the self-powered sensors directly to convert mechanical energy of the airflow into electricity. One of the major goals of the self-powered sensors and systems is realizing health monitoring and diagnosis. The relationship between the output signals and the models of respiratory diseases has not been studied deeply and clearly. Therefore, how to find an accurate relationship between them is a challenging and significant research topic. This review summarized the recent progress of the self-powered respiratory sensors and systems from aspects of device principle, output property, detecting index and so on. The challenges and perspectives have also been discussed for reference to the researchers who are interested in the field of self-powered sensors.

1. Introduction

Respiration plays one important role in vital signs for humans, by which can reflect changes in health status and prevalence of respiratory diseases like asthma, sleep apnea syndrome, pneumonia and tracheitis (Alkhouri et al., 2013; Buszewski et al., 2007; Haick et al., 2014; Hashoul and Haick, 2019; Paredi et al., 2000). Recent wearable and implantable sensors have played a vital role for detecting respiration parameters, such as respiratory rate and intensity, temperature and some special gas molecules of the exhaling air (Gandevia and McKenzie, 2008; Hoffmann et al., 2011; Kano et al., 2019; Li et al., 2018; Su et al., 2020b; Xu et al., 2021a). Among them, both of active and passive sensors shows their unique advantages in respiration monitoring (Cho et al., 2021; Li et al., 2021b; Xu et al., 2021b). The commercial and conventional respiration monitoring devices and systems have some disadvantages such as large size, bulky, expensive, which may restrict the application of daily use. How to measure respiration parameters by a continuous, convenient and comfortable way is a meaningful and useful research content. Researchers have developed some methods to improve the comfort and practicability of respiration monitoring, such as investigating noncontact monitoring strategy, using soft textile and so on (Cho et al., 2021; Zhou et al. 2020a, 2020b). Particularly, self-powered respiration sensors have attracted wide interest from scholars in the field of biomedical sensing (Ouyang et al., 2021; Zou et al. 2020, 2021). Self-powered devices can convert biomechanical or thermal energy of respiration into electricity directly, including triboelectric nanogenerator (TENG), piezoelectric nanogenerator (PENG), pyroelectric nanogenerator (PyNG), hygroelectric nanogenerator (HEG) and electromagnetic devices (Feng et al., 2018; Khandelwal et al., 2020; Luo et al.; Zhu et al., 2015; Zi et al., 2015). The output electrical signals of them have close relationship to the respiration parameters. For example, the TENG driven by air flow can generate pulses corresponding to the dynamic characteristics of the air flow (Guo et al., 2014; Wang et al., 2018).

Since the self-powered respiratory sensors based on polyvinylidene fluoride (PVDF) was demonstrated in 1990 (Chen et al., 1990), various achievements have been gained with the developments of material science and micro/nano-fabrication technology (Han et al., 2020; Wang et al., 2015a; Xie and Wei, 2014). Particularly, nanogenerators based on piezoelectric and triboelectric effects are promoting the self-powered

* Corresponding author. Beijing Advanced Innovation Center for Biomedical Engineering, Beihang University, Beijing, 100191, China.
** Corresponding author. Beijing Institute of Nanoenergy and Nanosystems, Chinese Academy of Sciences, 101400 Beijing, China.
E-mail addresses: bjshi@buaa.edu.cn (B. Shi), zli@binn.cas.cn (Z. Li).

https://doi.org/10.1016/j.bios.2021.113609
Received 6 July 2021; Received in revised form 26 August 2021; Accepted 31 August 2021
Available online 7 September 2021
0956-5663/© 2021 Elsevier B.V. All rights reserved.

respiration sensors and systems evolving into smaller, lighter, more sensitive and accurate, and more convenient for wearable and implantable scenarios (Fan et al., 2016; Tricoli et al., 2017; Wang, 2012; Wang et al., 2015b). Scientists have advanced some reviews about nanogenerators using in bioengineering, mostly focus on the using and future trends of TENG for biomedical sensing including respiration monitoring (Lama et al., 2021; Tat et al., 2021; Zhang et al., 2021a; Zhao et al., 2021). Tai et al. reviews the evolution of breath analysis from the prospects of humidity and gas sensing (Tai et al., 2020). Moreover, Su et al. came up with a review about TENG enabled self-powered respiration monitoring recently, which clearly shows the sensing mechanism and theoretical model of both physical respiratory signals collecting and molecular breath analysis (Su et al., 2021a). In these works, we can see that the respiratory sensor based on nanogenerator plays a vital role in the development of active self-powered biosensing because of the advantages such as small size, high biocompatibility, simple structure, easy

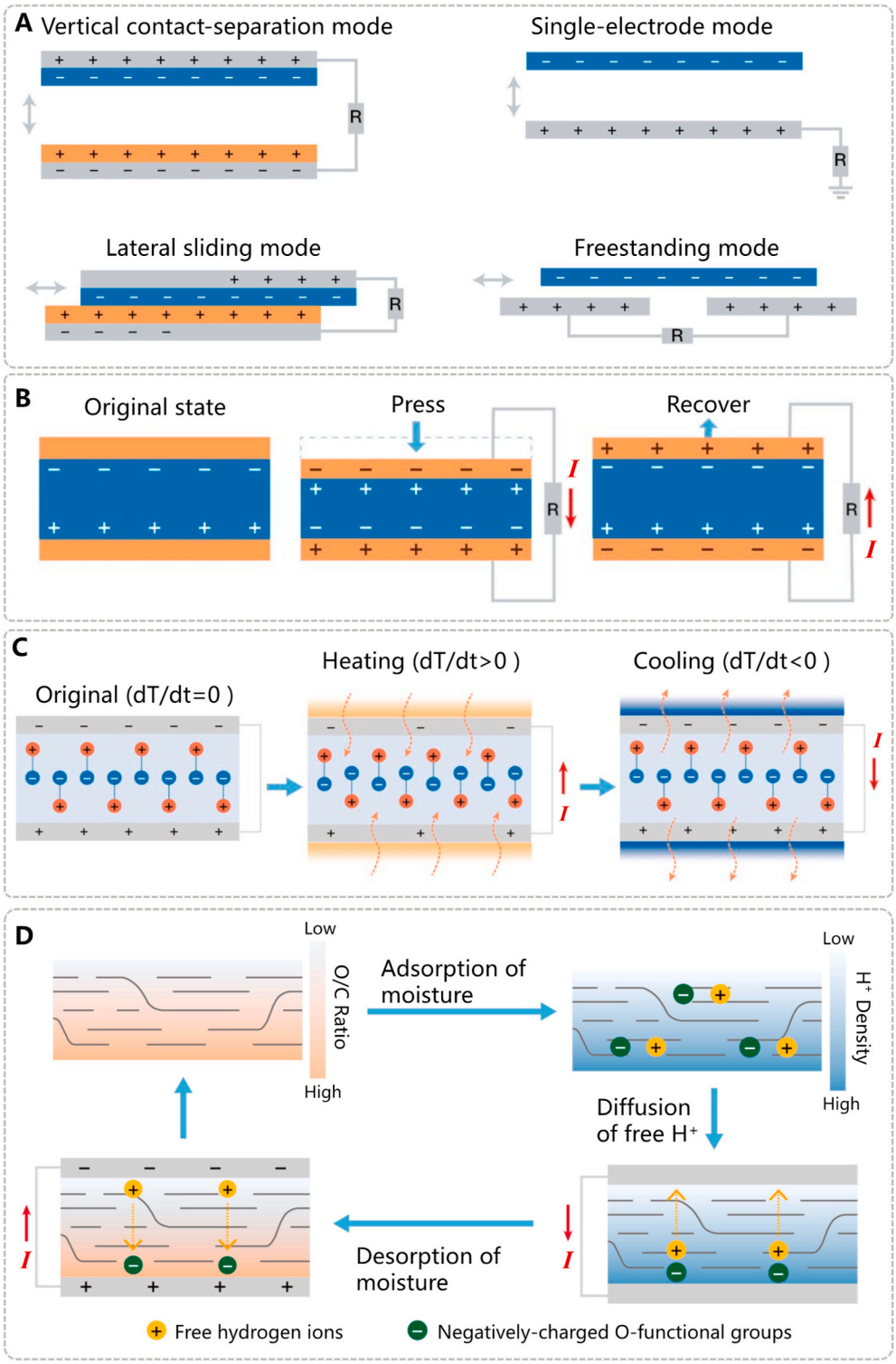

Fig. 1. The working mechanisms of self-powered respiration monitoring systems
(A) Four working modes of TENG. (B) Schematic diagrams based on PENG. (C) Typical diagrams of pyroelectric effect. (D) Schematic diagrams of hygroelectric effect.

fabrication and wide applicability. Additionally, with the establishment of Internet of Things, these self-powered respiration monitoring systems would help in the communication of intelligent wireless sensor in the near future.

Here, we reviewed the developments of self-powered respiration monitoring devices and systems, from the aspects of device types, output performance, index of respiratory sensing, etc. The self-powered sensors can be driven by the exhale air through mouth, which can reflect the breath conditions directly. Moreover, researchers have developed self-powered temperature sensors based on pyroelectric materials and surface modified nanogenerators to detect gas molecules of the breath air. Meanwhile, we also presented challenges and perspectives of the self-powered respiration monitoring. Although many significant advances have been achieved, there are still some bottlenecks such as it is difficult to provide enough diagnostic information just according to outputs of the self-powered sensors so far. However, it is believed that we can get more information from the outputs of the self-powered devices with the help of artificial intelligence or some other embryonic novel methods to deal with the sensing signals.

2. Types of self-powered respiration sensors

Typical self-powered respiration sensor systems can be divided into six categories: triboelectric, piezoelectric, pyroelectric, hygroelectric, electromagnetic and hybrid mode.

2.1. Triboelectric

Triboelectric effect (TE) is one of the most common phenomena existing in daily life. Although has been proved exist for far too long, scientists took centuries to study TE systematically (Lodge and Bhushan, 2007; Logan and Taylor, 1930; Wang and Wang, 2019). TE was always be deemed as an adverse effect, which can hardly be applied to practical applications. Until 2012, Wang's group invented triboelectric nanogenerator (TENG) (Fan et al., 2012). TENG became a reliable source to transform mechanical signal into electrical output. Since the rapidly development of researches in recent years, TENG has been proved to have significant advantages such as high output, easy to manufacture, low cost, light weight, and stability (Chao et al., 2020; Chen et al., 2020b; Jiang et al., 2018; Liu et al., 2019a; Shi et al., 2019). Moreover, there are more and more works based on using TENG as the self-powered biomedical sensor lately (Chen et al., 2021; Yang et al., 2015; Zhang et al., 2021c).

Based upon the difference of working mechanisms, TENG can be split into four basic working modes (Wang, 2017): vertical contact-separation mode (Wu et al., 2017), lateral sliding mode (Zhang et al., 2019b), single-electrode mode (Shin et al., 2018), and freestanding mode (Wang et al., 2014) (Fig. 1A). The vertical contact-separation mode utilizes periodic contact and separation between two triboelectric layers with distinct electron affinity to induce electron flow in electrodes. With simple structure, this mode is easy to design and achieve, but usually has difficulty in packaging for the changing volume of the spacer. The lateral-sliding mode is considerably alike the vertical contact-separation mode, except for the mechanical force is applied to the contact surface in parallel. Compared with vertical contact-separation mode, this working mode can harvest mechanical energy from different directions, but may be harmful to the robustness and durability. Other than the former two working modes, single-electrode mode just has one freely movable electrode. While the other electrode is connected to ground through a load, single-electrode mode is guaranteed more flexible but less stability and output. However, the freestanding mode keeps two electrodes relative stable and connect with each other through the load. With dielectric segment moving between two electrodes, a charge transfer between electrodes gets induced. This mode always applied in sliding motion detecting, like airflow and water flow. For the respiration monitoring sensor, the vertical contact-separation mode is the widest used and the most suitable one (Han et al., 2020; Kim et al., 2019; Wu et al., 2017).

2.2. Piezoelectric

The basic principle of PENG is breaking the central symmetry of crystal structure of piezoelectric materials caused by external force (Bai et al., 2018; Shin et al., 2020; Zheng et al., 2021a). In the undisturbed state, the charge centers of cations coincide with anions. When external force applied on them, the structure of piezoelectric materials would deform, result in the positive and negative charge centers being separated to form a piezoelectric potential. If connected with an external load, the deformed crystal would drive the free electron through external circuit, then realize new equilibrium state (Fig. 1B). The basic principle and model of PENG are suitable for lead zirconate titanate (PZT), $BaTiO_3$ (BTO), polyvinylidenefluoride (PVDF), poly(vinylidene fluoride-trifluoroethylene) (P(VDF-TrFE)), zinc oxide (ZnO) and some other piezoelectric materials (Lee et al., 2018; Park et al., 2014; Raj et al., 2018; Zhang et al., 2020). Among them, the self-powered piezoelectric respiration sensors usually chose flexible materials like PVDF and P(VDF-TrFE) considering the comfort sensation of users (Chen et al., 2015; Yang et al., 2020). Since the most important components of PENG are the piezoelectric materials and the flexible substrate, material selection and structure design are the core factors of its development (Bodkhe et al., 2018; Song et al., 2020; Su et al., 2021b; Yang et al., 2020).

2.3. Pyroelectric and hygroelectric

Wasted heat is a common energy source, which abounds in our living environment (Ryu and Kim, 2021; Zhou and Zhao, 2017). By developing PyNG with pyroelectric materials like PVDF, harvesting and reusing of wasted heat can be achieved (Newnham et al., 1978; Wang et al., 2016). The working mechanism of the PyNG driven by human respiration is illustrated in Fig. 1C. At room temperature, the equilibrium state of the electric dipoles in polarized pyroelectric material would induce constant negative and positive charges, respectively at the top and bottom electrodes. When ambient temperature raised, the dipole moments would lose their orientation, thus reduced the polarization density of the material. The decrease of the polarization results in a decrease of free charges within the material surface, thus induces current in external circuit between electrodes under short-circuit state. In contrast, low temperature could cool the PyNG and strengthen the dipole moment, then induce reversed current. The temperature and moisture of human breathing would bring or take the heat from pyroelectric materials, which generate output signals correlated with respiratory states (Sultana et al., 2018; Sun et al., 2018; Xue et al., 2017).

The hygroelectric effect is an energy conversion process that transform the potential energy of water molecules into electricity. Qu's group found that the single graphene oxide film (GOF) with a preformed oxygen-containing group gradient (so called gradient GOF, g-GOF) can convert the energy of moisture into electricity through the moisture-electric energy transformation (MEET) (Liang et al., 2017; Zhao et al., 2015). The fundamental mechanism of hygroelectric effect was illustrated by the schematic in Fig. 1D. Because of the oxygen-containing groups (e.g., –OH, –COOH) gradient in g-GOF, the moisture molecules would be adsorbed and form a concentration gradient of free H^+. The diffusion of H^+ under the driven of concentration gradient can lead to free electron movement of external circuit. In turn, this induced electric field would impel H^+ to migrate back to its high concentration side. Subsequently, with the desorption of water molecules, the diffusion of H^+ driven by concentration gradient got weakened, thus resulted in a reverse electron movement of external circuit. Most of the hygroelectric sensor system was based on graphene and its derivatives, driven by moisture tide generated by human breath, they can sensitively monitor respiration states without external energy supplies (Ye et al., 2016;

Zhang et al., 2020).

2.4. Electromagnetic/hybrid and others

There are some other kinds of self-powered respiration sensors, such as electromagnetic and hybrid (Shahhaidar et al., 2013; Xia et al., 2015; Zhu et al., 2020). Based on the electromagnetic effect, the respiration sensors mostly require rigid structure to maintain interaction between the magnet and conductive coils, which mains relatively large size and high weight (Beeby et al. 2006, 2007). The electromagnetic respiration monitoring device can convert the linear displacement change of chest or abdomen circumference into electrical energy. Compared to flexible nanofiber-based PENG, it may lack of flexibility but usually have higher efficiency. However, under the same vibration circumstance smaller than 5 Hz, the output of electromagnetic effect-based generator is considerably lower than TENG (Wang et al., 2017b; Zi et al., 2016). Other than the conventional structure of rigid electromagnetic sensor system, there some methods to improve the flexibility, such as replacing magnet and metal coils by magnetic powders and liquid metal (Zhang et al., 2021b). Due to the potential to detect multiple types of respiratory signals, the hybrid respiration monitoring techniques have been broadly evolved for the past few years (Kim et al., 2019; Zhu et al., 2020). Based on hybrid mechanisms such as pyroelectric and piezoelectric, triboelectric and piezoelectric, pyroelectric and electromagnetic et al. (Mahbub et al., 2017; Zi et al., 2015), these kinds of respiration sensor may have more function than onefold self-powered respiration sensors, but also more complicated structures and larger size. For example, to combine the higher output voltage of triboelectric generator with the higher output current of electromagnetic generator, Xia et al. proposed a novel triboelectric-electromagnetic generator which has great response to the breath (Xia et al., 2015). Except for above types, there remains some respiration sensors such as electrostatic sensor based on electrets (Cheng et al., 2017b; Lin et al., 2019). They need to be pre-charged before using, but it also suffers inevitable decay of implanted surface charge.

3. Applications of self-powered respiration monitoring system

For a long time, the cognition stage of respiration monitoring system only stayed in active sensors with limited functionality and bulky size. In 2011, Roopa et al. firstly came up with the conception of "self-powered breath sensor", using PVDF film in cantilever configuration as the sensing element (Roopa et al., 2011). The application of self-powered respiration monitoring system developed sharply thereafter. Classified by function, they can be mainly divided into three parts: respiratory mechanical signal collecting, breathing temperature/humidity monitoring, and molecular detection of exhaled gas (Han et al., 2020; Kim et al., 2019; Zhao et al., 2017). Categorized by working modes, they principally include implantable and wearable respiratory monitoring systems (Liu et al., 2019b; Ma et al., 2016; Yang et al., 2020).

3.1. Respiratory mechanical signal collecting

Our respiratory process induces the change of several mechanical signals, such as the movement of chest and the air flow of inhalation/exhalation process (Amann et al., 2014; Bruderer et al., 2019). However, the working mechanism of most self-powered respiratory monitoring systems is based on translating these mechanical signals into pressure signals, then detecting the variation of pressure signals (Fig. 2A) (Chen et al. 2015, 2017b; Chun et al., 2020; Wang et al., 2017a; Zhang et al., 2020). For more intuitive presenting of the self-powered respiration sensor systems for respiratory mechanical signal collecting in recent years, Table 1 summarized their main materials, size and output characteristics by different sensor positions. The position of the respiratory sensor influences most in the mechanical signal collection, cause different position decides whether it been driven by body movements or air flow. Sensors deployed in areas of abdomen, chest and throat are mainly driven by the body movements. Due to the relatively large movements, they normally have higher output than others driven by breath air flow. However, the most temperature, humidity and molecules detection are realized by respiration monitoring systems placed around the nose and mouth gathering the exhaled gas. The implanted respiratory sensors are mostly used to harvest energy and detect mechanical signals.

Based on monitoring the direct change of contact pressure, Bai et al. reported a new membrane-based triboelectric sensor about pressure sensing in 2014, which has resolutions of 0.34 Pa and 0.16 Pa corresponding to the increase and decrease period of air pressure, respectively (Fig. 2B(i)-(iii)) (Bai et al., 2014). The periodical contact/separation between the latex membrane and fluorinated ethylene propylene (FEP) film can reflect the pressure change induced by footstep, respiration and heartbeat. When connected with an air bag and attached to the abdomen of a subject, the system can realize self-powered respiration monitoring in real time (Fig. 2B(iv)). Based on the microsphere-based TENG, Liu et al. developed an ultrasensitive human respiration monitoring system with pressure sensing capacity (Liu et al., 2019b). The most important component of this TENG is the triboelectric thin layer made by thermally expandable microspheres and polydimethylsiloxane (PDMS) (Fig. 2C(i)). As shown in Fig. 2C(ii), different pressures result in different contact areas, and thus different triboelectric surface charges. When attached to the chest of subject, this 33×33 mm^2 sensitive pressure sensor can output correlate signals in response to each breathing states (Fig. 2C(iii)). The signal recorded showed significant differences between the shallow and deep breath state, with the respiratory rates of 30 and 9 breaths/minute, respectively. Moreover, the microsphere-based sensor can also be used in detection of the wrist pulse, which would bring us more vital signs by noninvasive medical diagnosis.

Most of the respiratory mechanical signal monitoring systems are based on the direct contact between the electronics and subjects (Cheng et al., 2017a; Rao Alluri et al., 2018; Sadri et al., 2019; Zhang et al., 2020). However, Chen et al. noticed vacancies on the researches of noncontact respiratory sensors, so they developed a hollow microstructured (HM) self-powered pressure sensor (SPS) that realized information collecting of breath process without direct skin contact (Fig. 2D(i)) (Chen et al., 2018). Its working mechanism can be principally summarized as the electrostatic phenomena happening between the negatively charged FEP/Ag layer and ethylene-vinyl acetate (EVA)/Ag layer. Working under the pressure of body weight, the HM-SPS can sensitively monitor the respiratory state as well the heartbeat in a noncontact mode, as shown in Fig. 2D(ii). Corresponding to various successive movements of the healthy subject, the outputs have significant different performances (Fig. 2D(iii)). The development of noncontact HM-SPS improved the experience of user comfort, which promoted the update of sleep-based health monitoring equipment.

In above, we can find that researchers have developed considerable self-powered respiration monitoring devices through direct skin contact. Most of them are based on the mechanical signal collecting around the chest, abdomen and throat. The direct contact with skin in these parts guaranteed the respiration sensor can be driven by the body movement induced by breathing, and collecting respiratory signals through the process. In general, the mechanical information detection of respiration monitoring through skin breathing is easier than mouth or nose breathing, because body movement is more powerful than air flow. Moreover, self-powered respiratory sensors can also drove by the air flow generated by breath behaviors. Wang et al. presented an air-flow-driven TENG respiratory sensor, in which the flexible nanostructured polytetrafluoroethylene (n-PTFE) thin film would regularly vibrate in an acrylic tube when been exposed to the air flow (Fig. 2E(i)) (Wang et al., 2018). The TENG has correlative response to different breathing states, and the cumulative quantity of charge transferred in respiratory process has highly correlation with the total volume of exchanged gas (Fig. 2E

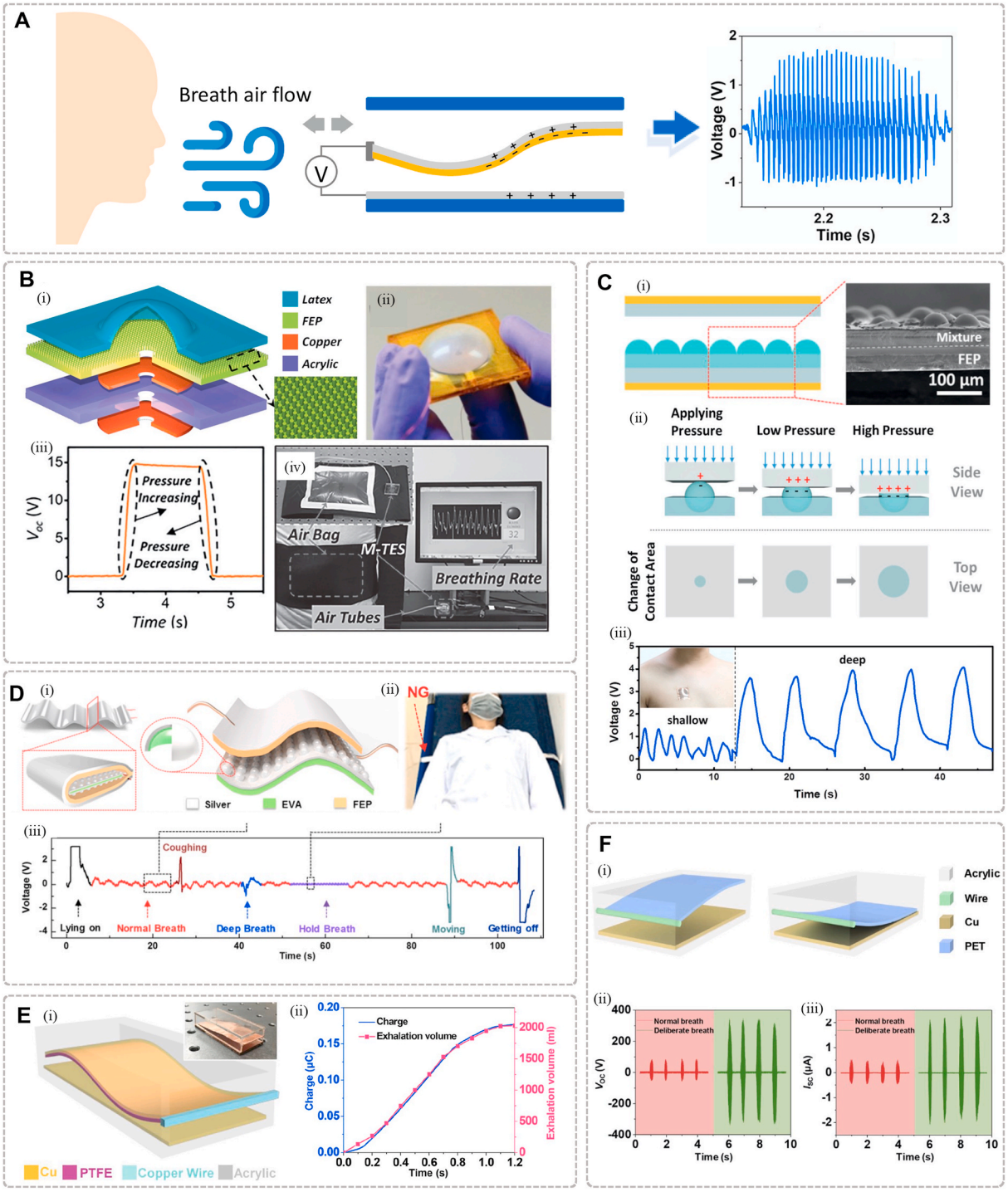

Fig. 2. Respiratory mechanical signal collecting

(A) Schematic diagram of the typical working process of the respiration monitoring system driven by airflow. (B) Schematic (i) and photograph (ii) of the M-TES. (iii) Magnified image of the output voltage signal. (iv) Display of respiratory signal detection by using the M-TES. Reproduced with permission, from ref (Bai et al., 2014), Copyright 2014, WILEY-VCH. (C) (i) Cross-sectional image of the PDMS layer. (ii) Deformation process. (iii) Voltage signals recorded during the respiratory rate detection. Reproduced with permission, from ref (Liu et al., 2019b), Copyright 2019, Elsevier. (D) (i) Schematic design of the HM monitoring system. (ii) Digital image of the HM-SPS underneath the subject. (iii) Electrical output signals of the HM-SPS related to successive motions. Reproduced with permission, from ref (Chen et al., 2018), Copyright 2018, American Chemical Society. (E) (i) Schematic configuration of the air-flow-driven TENG. (ii) The blue curve shows the accumulative charge, and the pink one shows the volume of gas carried in exhalation. Reproduced with permission, from ref (Wang et al., 2018), Copyright 2018, American Chemical Society. (F) (i) Schematic diagram of the TENG. (ii)-(iii) The output voltage (ii) and current (iii) of the TENG driven by the normal and deliberately strengthened breathing, respectively. Reproduced with permission, from ref (Zhang et al., 2019a), Copyright 2019, Elsevier. (For interpretation of the references to colour in this figure legend, the reader is referred to the Web version of this article.)

Table 1
A summary of recent self-powered respiration monitoring systems for respiratory mechanical signal collecting.

Sensor Positions		Main Materials	Size	Outputs	Ref.
around the chest/ abdomen/ throat	integrated in a chest belt	PZT, electromagnetic machine	\	V_M and power was ~0.5 V and about several mW	Shahhaidar et al. (2013)
	attached to the abdomen	latex, FEP	3.7 × 3.7 × 0.2 cm^3	resolutions of 0.34 Pa and 0.16 Pa when the air pressure increases and decreases, respectively	Bai et al. (2014)
	modified into a chest belt	electromagnetic rotary generator	arm length of R = 2.5 cm	maximum I_{SC}, V_{OC}, and power density of 32.2 μA, 500 V, and 2 mW for TEG, and 4.04 mA, 30 mV, and 15.8 μW for EMG, respectively	Xia et al. (2015)
	attached on the chest	FEP, PTFE	3 × 3 cm^2	sensitivity of 7380 pC N^{-1}, response time of 50 ms, low limit of detection of 5 Pa	Wang et al. (2017)
	attached to a belt around the abdomen	PDMS, PET	56 × 63 × 17 mm^3	V_{OC} of 16.8 V, maximum area power density of 7.584 mW m^{-2}	Vasandani et al. (2017)
	attached on the chest	P(VDF-TrFE), $BaTiO_3$	1 × 1 cm^2	peak output voltage of 13.2 V, average current density of 0.33 μA cm^{-2}	Chen et al. (2017a)
	placed around the belly	PDMS, P(VDF-TrFE)	2.5 × 3 cm^2	tribo- and piezo-electric peak power density reached up to 84 μW cm^{-2} and 0.11 μW cm^{-2}	Chen et al. (2017b)
	attached on the chest	PTFE	4 cm in length	peak voltage of 0.66 V, and peak output power density of 2.25 nW cm^{-2}	Cheng et al. (2017a)
	attached on the chest	PVDF	42 × 20 × 0.6 mm^3	V_{OC} of 1.5 V, I_{SC} of 400 nA	Liu et al. (2017)
	underneath the back of subject	FEP	2 × 35 cm^2	V_{OC} of ~110 V, and peak power outputs ~219.8 μW	Chen et al. (2018)
	placed under the back	carbon nanotube doped PDMS	30 × 30 cm^2	output V_M of 21.5 V	Ding et al. (2018)
	attached on the throat	$0.3Ba_{0.7}Ca_{0.3}TiO_3$–$0.7BaSn_{0.12}Ti_{0.88}O_3$ nanoparticles, PDMS	\	piezoelectric composite strip can generate output of 130 V/0.8 μA	Alluri et al. (2018)
	sewn into a t-shirt on the side of the thorax	PVDF	250–1.5 mm	maximum voltage of ~1 V	Bodkhe et al. (2018)
	attached on the chest	PDMS, FEP	33 × 33 mm^2	maximum sensitivity reaches 150 mV Pa^{-1}	Liu et al. (2019)
	attached on the chest	ethyl cellulose, polyamide 6	~3 × 3 cm^2	peak V_M generated by pitch of ~30 V	Sadri et al. (2019)
	fixed on the abdomen	PTFE	4 × 4 cm^2	stable surface potential of −270 V, peak power of 56.25 μW	Lin et al. (2019)
	modified into an abdominal belt	PTFE	5 × 5 cm^2	the output V_M of ~40 V and ~30 V during exhalation and inhalation, respectively	Zhang (2019b)
	attached on the pit of the stomach	PVDF	1 cm^2	approximately 2.8 × 10^{-2} V kPa^{-1} within 1 kPa	Chun et al. (2020)
	attached on the chest	PVDF, ZnO	~2 × 1 cm^2	V_{OC} of 2.33 V	Yang et al. (2020)
	mounted on the abdomen	PTFE/PDMS, fish gelatin	5 × 5 cm^2	V_{OC}, I_{SC}, and output power density reach up to 130 V, 0.35 μA, and 45.8 μW cm^{-2}	Han et al. (2020)
around the nose/ mouth	put under the nose	P(VDF-TrFE)	10 × 10 mm^2	V_M of ~4.8 V, maximum current density of ~0.11 μA cm^{-1}	Chen et al. (2015)
	integrated with a mask	PEI electret	~5 × 5 cm^2	the maximum peak power was ~4.9 μW	Cheng et al. (2017b)
	fixed near the breather valve of the mask	PVDF, Ag	4 × 6 cm^2	V_M and I_M of ~10 V and ~110 nA	Cao et al. (2018)
	embedded in a conventional medical mask	PTFE, Cu	5.5 × 2 × 1 cm^3	average peak values of the output voltage and current reached 2.4 V and 1.7 μA	Wang et al. (2018)
	attached at a commercial mask	$Bi_4Ti_3O_{12}$	400 μm × 7 cm	maximum V_{OC}, I_{SC}, and area power density of 60 V, 400 nA, and 18.5 mW m^{-2}	Raj et al. (2018)
	integrated with a mask	PET	0.5 × 2 × 3.5 cm^3	average peak values of V_{OC} and I_{SC} reached about 1000 V and 4.3 μA	Zhang et al. (2019)
	near the nose	PDMS, silk fibroin	10 cm^2	the output V_M, I_M and power density of 666 V, 174.6 μA, 412 μW cm^{-2}	Wen et al. (2019)
	attached onto a mask	PU, P(VDF-TrFE)	4 × 2 cm^2	peak-to-peak output voltage of 23 V	Alam et al. (2020)
	integrated with a face mask	DF-CNF, FEP	4.9 cm^3	maximum V_{OC} and I_{SC} reaches 388 V and 18.6 μA, under the vertical force of 8 N and frequency of 5 Hz	Rajabi-Abhari et al. (2021)
	combined with a mask	PDMS, PVDF	~50 cm^2	pressure sensitivity of 54.37 mV kPa^{-1} and 9.80 mV kPa^{-1} under the range of 0–80 kPa and 80–240 kPa, respectively	Zhu et al. (2020)
	connected with a respirator above the face	$Nd_2Fe_{14}B$/liquid metal	45 × 45 × 11 mm^3	pressure-sensitivity up to 17.73 kPa^{-1}	Zhang et al. (2021)
implanted in vivo	implanted into the pericardial sac	PTFE, Al	30 × 20 × 1 mm^3	V_{OC} of ~10 V, I_{SC} of ~4 μA	Ma et al. (2016)
	implanted into the abdominal cavity	PTFE	1.1 × 3.5 × 0.8 mm^3	voltage up to 2.2 V	Li et al. (2018)
	set between the heart and pericardium	PTFE, Al	25 × 10 × 1.5 mm^3	V_{OC} of 14 V, I_{SC} of 5 μA	Zheng et al. (2016)
	implanted under the left chest skin	Kapton, Al	1.2 × 1.2 cm^2	Voc of 12 V and Isc of 0.25 μA	Zheng et al. (2014)

*Open-circuit voltage (V_{OC}), short-circuit current (I_{SC}), maximum voltage (V_M), maximum current (I_M), lead zirconate titanate (PZT), fluorinated ethylene propylene (FEP), triboelectric generator (TEG), electromagnetic generator (EMG), polytetrafluoroethylene (PTFE), polydimethylsiloxane (PDMS), polyethylene terephthalate

(PET), poly(vinylidene fluoride-trifluoroethylene) (P(VDF-TrFE)), polyvinylidene fluoride (PVDF), polyetherimide (PEI), polyurethane (PU), diatom frustule (DF), cellulose nanofibril (CNF), Aluminum (Al).

(ii)). Integrated with a transmitter and a signal processor, they realized a wireless real-time respiration monitoring system on account of the original air-flow-driven TENG. Zhang et al. then developed a breath-driven human-machine interaction (HMI) system basing on a single-electrode-mode triboelectric nanogenerator driven by airflow (Zhang et al., 2019a). The system has a structure resembles last one, however, with polyethylene terephthalate (PET) as the triboelectric material (Fig. 2F(i)). Except for delivering command controlled by breathing signals to realize HMI, this system can monitor respiration process such as distinguishing the deliberate breathing from normal breathing (Fig. 2F(ii)-(iii)).

3.2. Respiratory temperature/humidity monitoring

Except for the mechanical energy, human breathing possesses thermal energy and moisture content (Carpagnano et al., 2017; Sultana et al., 2018; Zhao et al., 2020). As shown in Fig. 3A, based on harvesting these signals, some self-powered respiration monitoring systems realizing respiratory temperature/humidity monitoring. Xue et al. developed a wearable breathing sensor based on the pyroelectric characteristic of PVDF, which can be driven by the respiration (Fig. 3B (i)) (Xue et al., 2017). The temperature difference generated from human respiration and ambient environment can induce correlated output electrical signals of the pyroelectric breathing sensor. Mounted on the respirator, this system shows high sensitivity to different breathing states (Fig. 3B(ii)). In addition, the pyroelectric respiratory sensor could be used for ambient temperature monitoring, because of its good linear dependence with room temperature (Fig. 3B(iii)). In 2019, Roy et al. developed a graphene-based piezo- and pyro-electric nanogenerator (GPPNG) with highly flexibility (Roy et al., 2019). The GPPNG consists of graphene oxide (GO) encapsulated PVDF nanofibers with a lowest limit of detection on pressures as 10 Pa and sensitivity up to 4.3 V/kPa (Fig. 3C(i)). It also has a pyroelectric output power density top out at 1.2 nW/m^2 under the periodic thermal fluctuations result from continuous human respiration, which indicates the potential of being a pyroelectric breathing sensor (Fig. 3C(ii)-(iii)).

Most of the self-powered humidity sensors for respiration monitoring are in dependence on the hygroelectric effect of GO, reduced graphene oxide (RGO) and so on (Feng et al., 2020; Zhang et al., 2020). In 2015, Zhao et al. firstly put forward a self-powered humidity sensor for respiration monitoring, which realized MEET based on the GOF (Zhao et al., 2015). The working mechanism of GOF generating electric power from moisture was so called hygroelectric effect later (Huang et al., 2018b; Yang et al., 2019). Using the moisture electric annealing (MeA) strategy to prepare single GOF, it would form oxygen-containing group gradient. When the g-GOF exposed to moisture, the generated concentration gradient of H^+ would induce potential and free electron movement along external circuit. Due to the high sensitivity to moisture signals, they built a self-powered respiration monitoring system to harvest the energy of breath (Fig. 3D(i)-(ii)). The output voltage and current can reach up to ~18 mV and ~5.7 μA cm^{-2}, respectively, during the calm breathing process of a healthy male subject (Fig. 3D(iii)-(iv)). Besides, the g-GOF could monitor the respiratory frequency along with heartbeat of a healthy subject after different intensity of exercise (Fig. 3D(v)). Afterwards, their group proposed a moisture powered potential switching based on GO nanoribbon network assemblies (Zhao et al., 2017). The resulting flexible membrane achieved respiration powered write and read, with long term stability and extremely low error risk (ON/OFF ratio of 106). Besides, they also developed a respiration-detective battery based on GOF and lithium foil (Ye et al., 2016). In this battery, the GOF captures and transfers the moisture, while the lithium foil triggers the redox reaction with the absorbed moisture. These work shows promising potential in using for future breath-based diagnostic biomedical sensor system.

Besides, there were also some researchers developed self-powered respiratory humidity sensors based on mechanisms different from the hygroelectric effect of the GO (Fang et al., 2020; Shen et al., 2020; Wang et al., 2019a; Wen et al., 2019; Xiao et al., 2019). Bošković et al. presented an aluminum-based humidity sensor for respiration monitoring, which has small volume and no need of external power supply. (Boskovic et al., 2020). Using the sputtered thin film of aluminum 1% silicon (Al 1% Si) as an interdigitated capacitor, the breath humidity sensor has similar working mechanism to aluminum-air battery (Fig. 3E(i)-(iii)). Been attached to the tube connected with a breathing mask, this sensor would give output signals in correlated with various paces (Fig. 3E (iv)-(v)). The experiments result shows this sensor has very fast response to humidity signals of respiration, with the reaction time as small as 10 ms and relaxation time in 50 ms. Afterwards, Li et al. developed a self-powered flexible respiration sensor based on polypyrrole modified melamine aerogel (PPy@MA) (Fig. 3F(i)-(ii)) (Li et al. 2020, 2021a). The porous structure and nanochannels in the PPy@MA promoted the adsorption and diffusion of water molecules. This sensor can be used to detect the moisture changes of the human skin and breath, due to the generated open-circuit voltage corresponding to various humidity level (Fig. 3F(iii)). When been placed in an environment with 98% relative humidity (RH), the PPy@MA humidity sensor generated the voltage of 105 mV, while the response and recovery time was 32 s and 13 s, respectively.

Here, Table 2 summarized main materials, size, sensor positions and output characteristics of the self-powered respiration sensor systems for respiratory temperature/humidity monitoring in recent years.

3.3. Molecular detection of exhaled gas

Breathing is one of the most important physiological process to exchange matters between the human body and ambient environment, including humidity, temperature, gas molecules and so on. Some of the gas species of exhalation (so called volatile organic compounds, VOCs) may have connection with certain diseases (de Gennaro et al., 2010; Hashoul and Haick, 2019; Paredi et al., 2002; van de Kant et al., 2012), for example, nitrogen oxides (NOx) is a gas marker of respiratory tract inflammatory diseases (Barker et al., 2006); acetone is related to diabetes (Pasquel and Umpierrez, 2014); and ammonia is connected with hepatitis (Bernal et al., 2010). Besides, the alcohol concentration of the breathed-out gas plays a vital role in identifying drunk driver, and also be recognized as an indicator of fatty liver (Chan et al., 2020; Solga, 2014). Some of the gas molecular from exhalation have been detected by the self-powered respiratory sensors successfully, which provides a potential way to enhance the properties of the respiration monitoring systems and strengthen the bonds between breathing signals and disease diagnosis (Fig. 4A). Here, Table 3 summarized the gas molecular types, main materials, size, sensor positions and output characteristics.

The carbon dioxide (CO_2) concentration can be used to distinguish inhale from exhale process. Kim et al. using a three-dimension printed triboelectric respiration sensor (TRS) to detecting breathing signals in real time, which contains a willow-like fluorinated ethylene propylene (FEP) film coated with polyethylenimine (PEI) (Fig. 4B(i)) (Kim et al., 2019). By analyzing the output voltage, they can recognize four respiratory modes, include strong, weak, long, and short. The output voltage of strong mode was almost triple than weak one, while the short and long respiration case have same output pattern in 0.5 s with difference of peak value. Innovatively, they utilize the PEI as the CO_2-capture material to distinguish expiration from inspiration because of the differences in CO_2 concentrations. As demonstrated in Fig. 4B(ii), at a relative humidity of 37%, the output voltage of TRS diminished by 11.73% after the CO_2 gas injection at a velocity of 6.5 m/s over a sustained period of time.

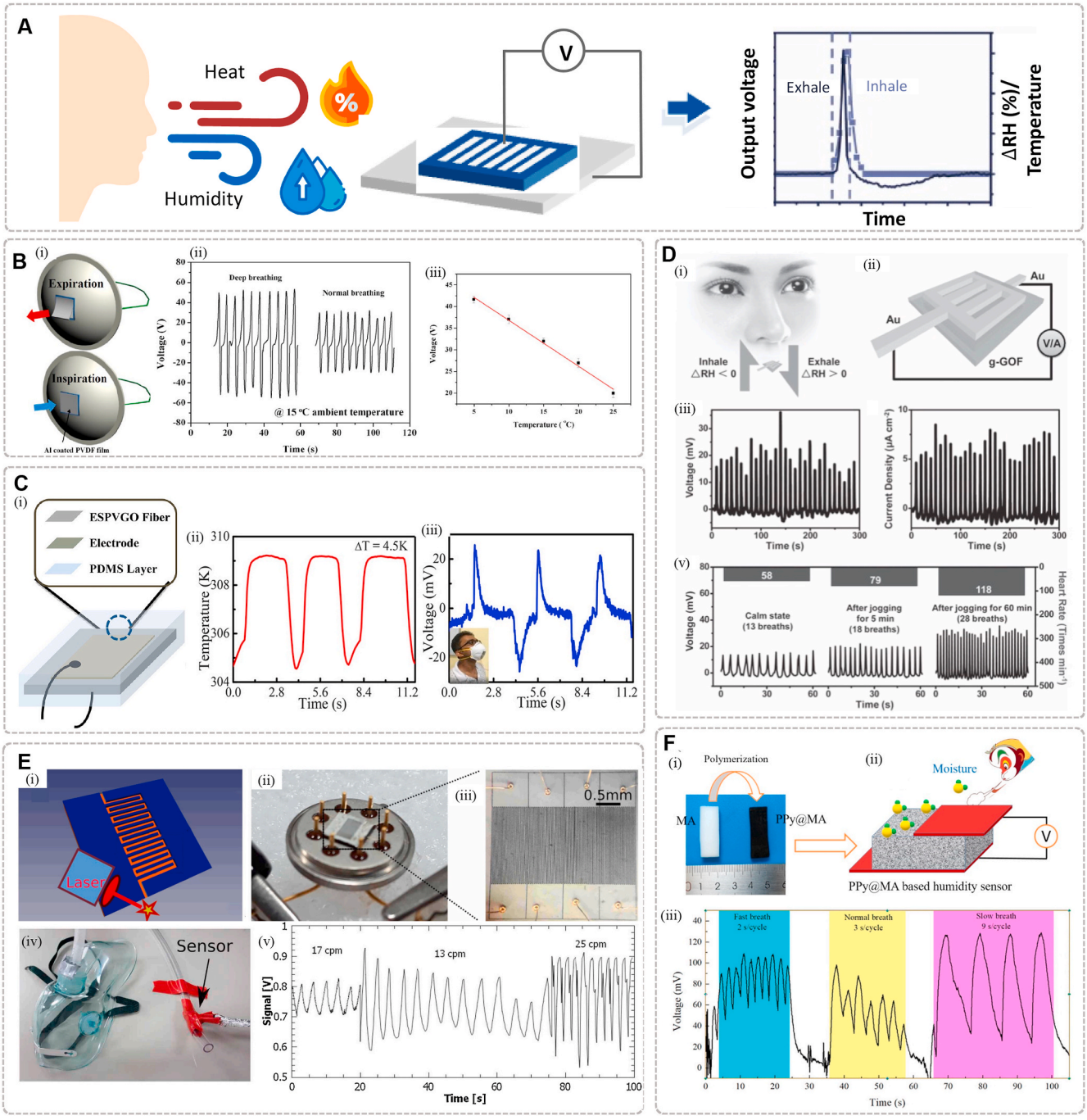

Fig. 3. Breathing temperature/humidity monitoring.
(A) Schematic diagram of the typical working process of the respiratory temperature/humidity monitoring system. (B) (i) Schematic of the PyNG breathing sensor. (ii) The output voltage of deep breathing and normal breathing. (iii) Plot and the linear fit of the open-circuit voltage versus the ambient temperature. Reproduced with permission, from ref (Xue et al., 2017), Copyright 2017, Elsevier. (C) (i) A sketch of the nanogenerator structure. (ii) The temperature fluctuation and (iii) recorded open circuit voltage of the GPPNG under the human respiration. Reproduced with permission, from ref (Roy et al., 2019), Copyright 2019, American Chemical Society. (D) (i) Schematic of the MEET device. (ii) The working structure of the MEET device. (iii) Voltage and (iv) current output generated by respiration during ΔRH of 21%. (v) Self-powered monitoring of respiratory frequency corresponding to heart rate after different exercise levels. Reproduced with permission, from ref (Zhao et al., 2015), Copyright 2015, WILEY-VCH. (E) (i) The demonstration of direct laser writing. (ii) Picture of the finished sensor. (iii) The surface of sensor. (iv) The breathing mask with the sensor attached at the end of the tube. (v) The output during breathing with different paces. Reproduced with permission, from ref (Boskovic et al., 2020), Copyright 2020, Elsevier. (F) (i) Photograph of MA and PPy@MA. (ii) Diagram of the working process of PPy@MA based humidity sensor. (iii) Response voltage of the humidity sensor based on PPy@MA under various respiratory frequency. Reproduced with permission, from ref (Li et al., 2020), Copyright 2020, Elsevier.

Table 2
A summary of recent self-powered respiration monitoring systems for respiratory temperature/humidity monitoring.

Sensor Positions		Main Materials	Size	Outputs	Ref.
directly placed around the nose/ mouth	placed under the nose	GOF	0.5 × 0.5 cm^2	V_{OC} of 35 mV with power density of 4.2 mW m^{-2}, energy conversion efficiency up to ~62%	Zhao et al. (2015)
	placed under the nose	Li, GOF	~4.68 cm^2	a capacity of 36.4 mA h cm^{-2}, maximum V_{OC} of 2.7 V and a maximum I_{SC} of ~16000 μA cm^{-2}	Ye et al. (2016)
	placed under nose or mouth	a commercial transducer	7 cm^2	V_{OC} and I_{SC} up to 1.5 V and 1.5 μA, and power density of 0.034 μW cm^{-2}	Sultana et al. (2018)
	placed ~50 mm from the human nose	TiO_2 nanowires	~1 × 1 cm^2	response times of ~3.6 s and recovery times of ~14 s	Xiao et al. (2019)
	placed under the nose	[PPy or PANI]-coated 3D polyurethane sponge	~10 × 6 × 2.2 cm^3	peak V_M and power was ~1.8 V and about several mW	Fang et al. (2020)
	placed before the mouth	Mg, oxidized carbon nanofibers	ample = 1.8 cm^2, sample thickness = 100 μm	V_{OC} up to 2.65 V within 10 ms, and the average peak I_{SC} density is ~6 mA cm^{-2}	Feng et al. (2020)
	placed before the mouth	PPy@MA	2.0 × 0.5 × 0.5 cm^3	the V_{OC} of 105 mV, when under 98% RH	Li et al. (2020)
	placed under the nose	SnS_2/RGO, Au/PTFE	effective friction contact area is 50 cm^2	peak-to-peak voltage of 500V and maximum output power of 378 μW	Zhang et al. (2020)
integrated with mask/ nasal cavity	attached inside the infant nasal cannula	PVDF		1.2 V 1.8 μW	Mahbub et al. (2017)
	attached to a mask	GO fiber	3 × 7 cm^2	maximum V_{OC} and current density per unit can reach 355 mV and 1.06 mA cm^{-2}	Liang et al. (2017)
	mounted on the respirator	PVDF	3.5 × 3.5 cm^2	V_{OC} of 42 V and I_{SC} of 2.5 μA	Xue et al. (2017)
	mounted on a N95 mask	PVDF, GO	7 × 18 cm^2	a sensitivity of 4.3 V/kPa under 10 Pa, maximum output power density of ~6.2 mWcm^{-2}	Roy et al. (2019)
	attached to the underside of the nasal cavity	GO film	~12 × 8 mm^2	the response time of 5 s, the recovery time of 3.5 s, and the sensitivity was 22 mV/%RH	Wang et al. (2019a)
	attached at the end of the tube of the breathing mask	Al 1% Si	1.58 × 0.74 mm^2	V_M of 1.5 V with response time down to 10 ms	Boskovic et al. (2020)

*Relative humidity (RH), graphene oxide (GO), graphene oxide film (GOF), lithium (Li), reduced graphene oxide (RGO), aluminum 1% silicon (Al 1% Si).

The TRS realized human respiratory monitoring combined with CO_2 sensing, and promoted the development of self-powered breathing sensors with molecular detecting function.

The alcohol concentration of the breathed-out gas is a vital index for safety and drunk driving test. Wen et al. introduced a self-powered alcohol breath detector based on blow-driven triboelectric nanogenerator (BD-TENG) (Wen et al., 2015). It has wide sensing range of 10 to 200 ppm and rapid response/recovery time of 11 s and 20 s. Xue et al. developed a new flexible smelling electronic skin (e-skin), which could be driven by human respiration and indicate alcohol concentration of breath (Xue et al., 2016). With the PANI (polyaniline)/PTFE/PANI sandwich nanostructures, this e-skin combines triboelectric effect with gas-sensing ability (Fig. 4C(i)-(ii)). This self-powered system can be utilized for visually identifying drunken driver when an adult blows it (Fig. 4C(iii)-(iv)). Their group also developed a respiration sensor utilizing the PANI/PVDF piezo-gas-sensing arrays, in which five different sensing units have selectively responses in related with particular gas markers (Fu et al., 2018). Thereinto, this device is proved usefully for detecting ethanol concentration in the exhalations. These work all promoted the development of self-powered systems, and also greatly advanced the applicability of them.

The increase of ammonia (NH_3) concentration in exhale gas indicates some illness like kidney disease. In 2019, Wang et al. developed a Ce-doped ZnO-PANI nanocomposite film for energy harvesting from breath together with the detection of trace-level NH_3 concentration (Wang et al., 2019c). Afterwards, they established a triboelectric self-powered respiration sensor (TSRS) and adopted relevant theoretical model for human respiration analyzing, with NH_3 sensing function (Wang et al., 2019b). As illustrated in Fig. 4D(i), the Ce-doped ZnO works not only as triboelectrification layer but NH_3 sensing material in TSRS. When attached to chest with the exhale gas gathering system, TSRS could gathering energy and respiratory rhythm from the regular expansion and contraction of chest, realizing exhale gas monitoring (Fig. 4D(ii)). In the simulative respiratory atmosphere (97.5% RH), the increase of NH_3 concentration significantly improves the electric output of TSRS (Fig. 4D(iii)). Moreover, they investigated the selectivity between the NH_3 and another 6 typical disease markers. The result shows that TSRS have great selectivity on NH_3 gas under the moisture atmosphere of 97.5% RH (Fig. 4D(iv)). This work implies the competence of TSRS in monitoring trace level NH_3 biomarker in exhale gas, and distinguish various respiratory behavior like normal, deep, shallow and fast breath.

Nitrogen dioxide (NO_2), as a hazardous gas, is ubiquitous around us. Su et al. developed a wearable alveolus-inspired membrane sensor (AIMS) based on TENG for human respiration monitoring and NO_2 detection (Fig. 4E(i)) (Su et al., 2020a). The target gas in and out could drive the latex membrane to expand and shrink, respectively, thus induce electric potential difference between the membrane and sensing film. Using the tungsten trioxide (WO_3) composite film to realize gas-sensing, the AIMS reveals the excellent sensitivity up to 340.24% under NO_2 concentration of 80 ppm (Fig. 4E(ii)). Compared with other gas, the AIMS also shows superior selectivity of NO_2 sensing (Fig. 4E (iii)). Output of AIMS can reflect the differences on period and capacity of respiration. This work provides an innovative approach to detect toxic gas by combining respiration monitoring with NO_2 detection.

4. Implantable and wearable respiration monitoring systems

As living standards rise and academic level grow, the self-powered respiratory systems have the tendency to be more miniaturized, portable and multifunctional (Alam et al., 2020; Reid and Mahbub, 2020; Tao, 2019). The emergence and development of implantable and wearable respiratory sensors catered to the needs of the public (Sheng et al., 2021; Shi et al., 2020; Sun et al., 2020; Wu et al., 2016; Zhao et al., 2016). The above-mentioned self-powered respiration monitoring systems are most wearable electronics, integrated with face masks, abdomen or chest belts. However, the implantable sensors have unique advantages such as high accuracy and the ability to continuously

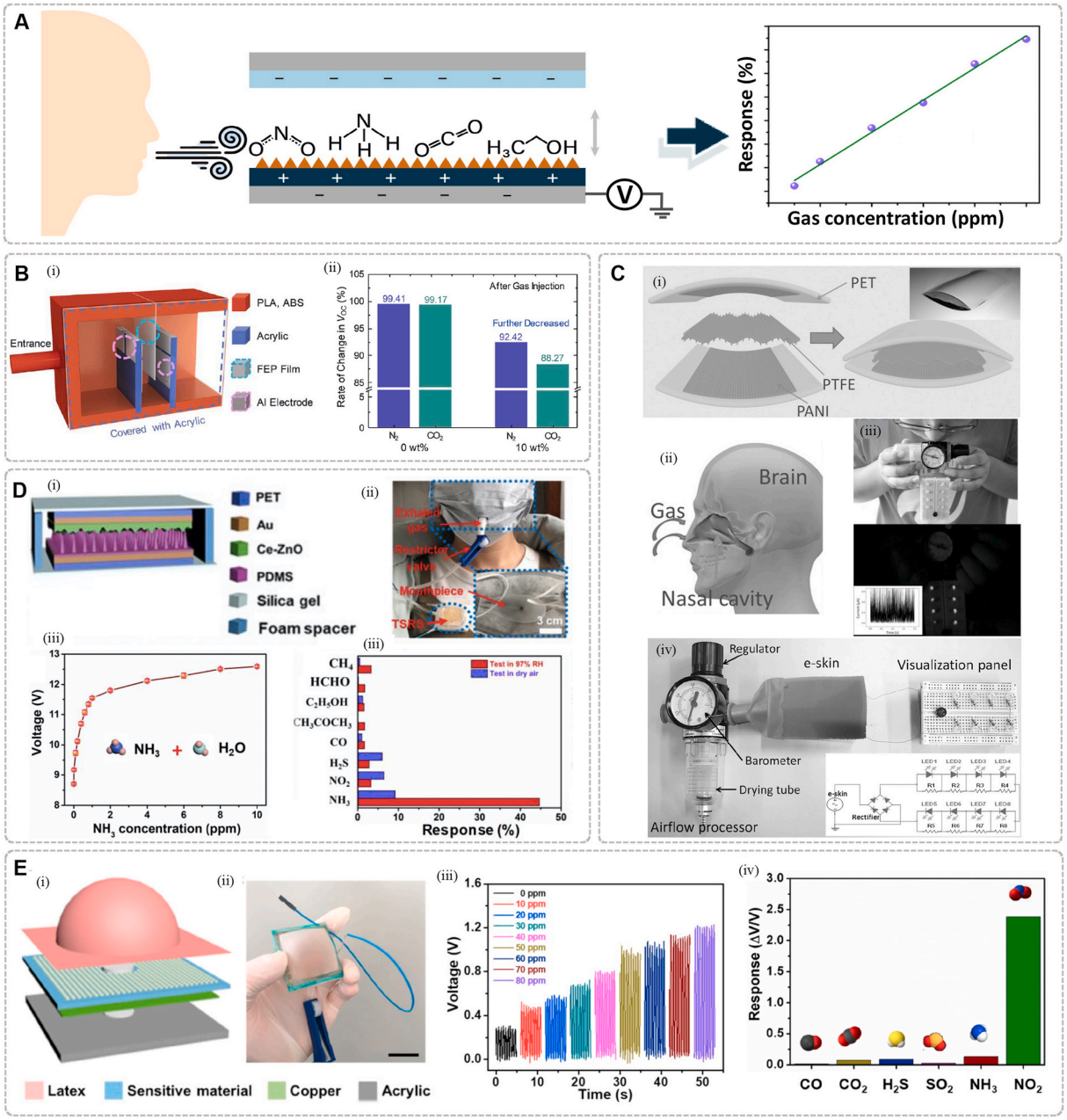

Fig. 4. Molecular detection of exhaled gas

(A) Schematic diagram of the typical working process of the respiration monitoring system detecting gas molecule. (B) (i) Container and inner structures of the TRS. (ii) The output voltages generated before and after CO_2 gas and N_2 gas injections. Reproduced with permission, from ref (Kim et al., 2019), Copyright 2019, Elsevier. (C) (i) Structure of the flexible smelling e-skin. (ii) The e-skin could be driven by gas flow (iii) Picture of the breath–alcohol visual monitoring system. (iv) The result shows that an adult can light 8 LEDs without drinking alcohol. Reproduced with permission, from ref (Xue et al., 2016), Copyright 2016, WILEY-VCH. (D) (i) Diagram of the TSRS. (ii) Photograph of the integrated wearable TSRS. (iii) Output voltage under 97.5% RH. (iv) Selectivity of TSRS under different humid atmosphere, respectively. Reproduced with permission, from ref (Wang et al., 2019b), Copyright 2019, Elsevier. (E) (i) Schematic of the structure of AIMS. (ii) Photograph of the AIMS. (iii) Dynamic response with 0.02 g NaOH treated WO_3. (iv) Selectivity of AIMS for NO_2 sensing. Reproduced with permission, from ref (Su et al., 2020a), Copyright 2020, American Chemical Society.

monitor target biomedical signals, because they are able to get closer to where physiological signals occur and avoid other interferences from body movements (Jiang et al., 2020; Zheng et al., 2014). Nevertheless, the progress of implantable monitoring devices subjects to the battery life (Huang et al., 2018a; Zheng et al., 2014).

The implantable self-powered respiratory monitoring system normally combines the function of energy-harvesting and respiratory signal collecting. Considering of the security and ethical issue of experiment, few studies about collecting respiratory signals were carried in vivo. However, quite a few related studies have been proved to be feasible in animal models. As flexible and integrated biomedical systems, they can harvest energy from contractile and relaxation motions of the heart, lung and diaphragm to realize respiratory sensing without external power supplies (Fig. 5A) (Dagdeviren et al., 2014). For example, Li et al. developed an implantable nanogenerator (i-NG) based on ultra-stretchable micrograting system, which provides a promising method for the evaluation of implantable medical devices (Fig. 5B(i)) (Li et al., 2018). After being implanted into the abdominal cavity of Sprague Dawley (SD) adult rats, it can harvest energy from the regular diaphragm movement during respiratory process, and output electrical

Table 3
A summary of recent self-powered respiration monitoring systems for molecular detection of exhaled gas.

Detection Content	Main Materials	Size	Sensor Positions	Outputs	Ref.
Ethanol	PTFE, PANI	5 × 4 × 2 cm^3	placed before the mouth and blows	the detection limit is 30 ppm, and the response is up to 66.8 against 210 ppm ethanol gas flow	Xue et al. (2016)
	PANI, PVDF	5 × 5 cm^2	placed before the mouth and blows	the output current before drinking beer is 8–12 nA	Fu et al. (2018)
	TiO_2 nanowires	several cm^3	located 1 cm from the mouth	output voltage of 0.5 V and maximum power density of 0.7 μW cm^{-2}	Shen et al. (2020)
NH_3	Ce-doped ZnO-PANI	6 × 4 × 2 cm^3	placed before the mouth and blows	NH_3-sensing ability has linearity of R^2 = 0.9928 and sensitivity of 13.66 ppm^{-1}	Wang et al. (2019c)
	Ce-doped ZnO, PDMS	3 × 3 cm^2	attached on the chest, with a conduit gathering exhaled gas	sensitivity of 20.13 ppm^{-1} to NH_3 at low concentration (0.1–1 ppm)	Wang et al. (2019b)
CO_2	PEI, FEP	\	placed before the mouth	peak V_M was ~15 V	Kim et al. (2019)
NO_2	WO_3 composite (gas sensing), Cu/latex (TENG)	~4 × 4 cm^2	integrated as gas test chamber and placed before the mouth	gas sensitivity shows linearity of 0.976, and over 20 times higher selectivity to NO_2	Su et al. (2020a)

*Polyaniline (PANI), nitrogen dioxide (NO_2), tungsten trioxide (WO_3), zinc oxide (ZnO), titanium dioxide (TiO_2), polypyrrole modified melamine aerogel (PPy@MA).

signals correlated with inhale and exhale part (Fig. 5B(ii)-(iii)).

Nowadays, the implantable monitoring electronic devices tend to be self-powered, one-stop and multifunctional (Sheng et al., 2021; Zheng et al., 2014). Ma et al. developed an implantable triboelectric active sensor (iTEAS) for real-time biomedical monitoring (Ma et al., 2016). It composed by triboelectric layers, electrodes and spacers, with all structures get sealed in a multilayer flexible shell (Fig. 5C(i)). Implanted into the pericardial sac, the iTEAS can not only monitor the respiratory rates in real-time, but also detect other physiological signs such as heart rhythm and blood pressure (Fig. 5C(ii)). During the breathing process, as shown in Fig. 5C(iii), the output peaks of the iTEAS increased from ~4.8 V to ~6.3 V when inhalation, and decreased to the original state when exhalation. Zheng et al. designed an implantable triboelectric nanogenerator (iTENG) with multilayered structure as a self-powered healthcare monitoring system (Fig. 5D(i)-(iii)) (Zheng et al., 2016). It can generate open-circuit voltage and corresponding short-circuit current up to 14 V and 5 μA, respectively, when driven by the heartbeat of a Yorkshire porcine. Besides, the iTENG has the output peaks consistent with the breath cycle (Fig. 5D(iv)). They also presented the work of iTENG using in harvesting energy from mechanical movements in breathing (Fig. 5E(i)-(ii)) (Zheng et al., 2014). After being implanted under the left chest of the rat, it can measure forced vital capacity of the rat (Fig. 5E(iii)-(iv)). The iTENG shows potential in developing the lifetime-implantable self-powered medical devices.

Compared with implantable self-powered sensors, wearable sensors tend to be more flexible and easier to update (Alam et al., 2020; Liao et al., 2020; Liu et al., 2019b; Wu et al., 2016; Yang et al., 2020). The wearable respiratory monitoring sensor can be integrated into an abundant of wearable products, such as face masks (Raj et al., 2018) and chest/abdomen belts (Chen et al., 2017a; Ding et al., 2018). Cheng et al. developed a self-powered wearable smart face mask, using the electrospun PEI nonwoven as electret materials (Cheng et al., 2017b). Based on the charges maintain ability of PEI under extreme moisture circumstance, the smart face mask can remove the sub-micron particulate matter more efficiently and harvest the energy from breath airflow. During the human breathe movements, the mask can be used as a self-powered biomedical sensor for monitoring respiratory rates. A healthy man breathed about 21 times/minute. Combined with a liquid crystal display, this system may have the potential to warn the decay of filtration efficiency. Qu's group reported a self-powered wearable hygroelectric system based on graphene fibers for respiration monitoring, gathering energy from environmental moisture through the MEET process (Liang et al., 2017). When attached onto a mask, with the maximum output voltage reaches to 292 mV, this device can tell the difference between different human breathing states. Rajabi-Abhari et al. introduced a diatom frustules (DFs) enhanced cellulose nanofibril (CNF)-based TENG for respiration monitoring, which can generate time-average power of 85.5 mW/cm^3 with efficient contact area of 4.9 cm^2 under contact-separation mode (Rajabi-Abhari et al., 2021). On account of this DF-CNF TENG, they developed a disposable self-powered smart mask. When human breathing, the airflow would make the FEP film fluttered between two DF-CNF layers, thus generated output voltage corresponding to respiratory states. The double-TENG-based breathing sensor has a higher maximum voltage compared with the single-TENG mode. Due to its biocompatible and high output, this sensor has potential in future wearable and skin-attachable health monitoring system.

Except for the development of smart face masks, there are certain works based on chest/abdomen belts, flexible textile and e-skin (Alam et al., 2020; Cao et al., 2018; Chen et al., 2020a; Chung et al., 2019; Liu et al., 2017; Zhao et al., 2016; Zhu et al., 2020). In 2013, Shahhaidar et al. used the harvester of the chest movements to collect human energy, which can also work as a self-powered respiratory biosensor (Shahhaidar et al., 2013). They designed piezoelectric and electromagnetic sensor/harvester systems embedded in the chest belt. Afterwards, they developed another optimized electromagnetic self-powered wearable sensor in 2015, which was also combined with the chest belt (Shahhaidar et al., 2015). By putting this sensor system on the xyphoid process and umbilicus, it can monitor the respiratory process by harvesting the energy generated in movements of the chest wall. Based on contact-separation mode, Vasandani et al. developed a microdome-patterned wearable respiratory energy harvester (wREH) (Vasandani et al., 2017). The delicate design of micro-patterned PDMS aims for the enhancement of the output performance of the wREH. With small size and light weight, the wREH can be attached to a noncompliant belt around the abdomen and used to track the rate and depth of respiration. Under the normal respiratory testing condition, the open-circuit voltage reaches up to 16.8 V, the maximum area power density of 7.584 mW m^{-2}. This wearable device can not only act as a self-powered sensitive sensor to monitor respiratory, but also harvest energy generated during breath process, which presents practical potential in future integrated biomedical sensor networks.

5. Conclusion and perspectives

With the growing advocacy of healthy and quality life, the progress of biomedical monitoring systems has been accelerated in recent years, including respiration monitoring systems. In Table 4, we systematically compared the advantages and challenges of recent self-powered respiration monitoring systems by different types of signals collection, and

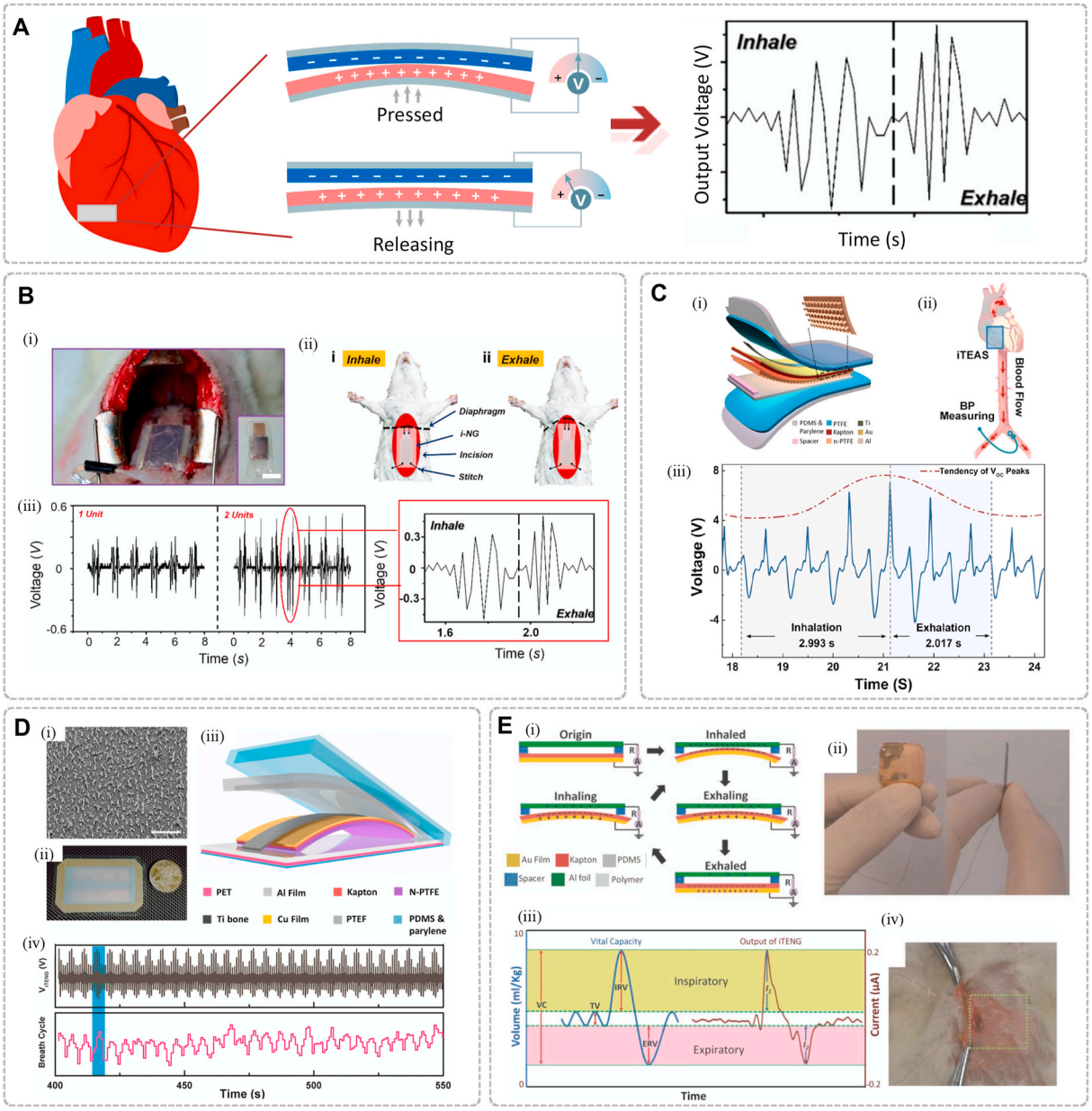

Fig. 5. Implantable respiratory monitoring system

(A) Schematic diagram of the typical working process of the implantable respiration monitoring system. (B) (i) Digital image of an i-NG implanted inside the abdominal cavity of a SD rat. (ii) Working process of the i-NG driven by diaphragm motion during respiration. (iii) In vivo voltage outputs measured from i-NGs with a single unit (left) and double unit (right). Reproduced with permission, from ref (Li et al., 2018), Copyright 2018, American Chemical Society. (C) (i) Exploded-view illustration and (ii) the working mechanisms of the iTEAS. (iii) Output during the process of inhalation and exhalation. Reproduced with permission, from ref (Ma et al., 2016), Copyright 2016, American Chemical Society. (D) (i) Scanning electron microscopy image of the PTFE film. (ii, iii) Schematic diagram and photograph of the iTENG. (iv) Output peaks of the iTENGs presented consistent with the breath cycle (blue box). Reproduced with permission, from ref (Zheng et al., 2016), Copyright 2016, American Chemical Society. (E) (i) Working principle of the iTENG. (ii) Digital picture of the fabricated TENG. (iii) Correlation between the output of iTENG and respiratory movements. (iv) An iTENG buried under the thoracic skin. Reproduced with permission, from ref (Zheng et al., 2014), Copyright 2014, WILEY-VCH. (For interpretation of the references to colour in this figure legend, the reader is referred to the Web version of this article.)

discuss the perspectives of them. The output of an air-flow-driven respiratory sensor has a closer relationship with the changes in flow, such as breath frequency, depth and the volume of air exchanged during respiration. While the respiration monitoring system based on pyroelectric and hygroelectric effect depends more on the temperature and humidity of exhaled gas, respectively, which means more susceptible to external influences. Moreover, the respiratory sensor about molecular detection can provide further information about the chemical composition, thus helpful in the diagnosis of certain diseases. Furthermore, with the convergence of various Internet of Things architectures, the programme of smart healthcare system has been accelerating the research on self-powered electronics (Ray, 2018; Zheng et al., 2021b). It is inspiring that the researches of self-powered respiration monitoring have developed rapidly. The overwhelming majority of self-powered respiration monitoring systems are based on gathering respiratory signals from nasal respiration, mouth breathing, and chest movement (Fig. 6). Among these physiological activities, the gas exhaled from nose and mouth mainly contains signals of airflow, humidity, temperature, and molecules, while the chest movement primarily provide mechanical signals like pressure changes. However, for the future development,

Table 4
The summary and comparison about advantages, challenges and perspectives of recent self-powered respiration monitoring systems for different types of signal collection.

Signals	Devices	Advantages	Challenges	Perspectives
Mechanical	Triboelectric	- Wide material chosen - High output voltage - Light and soft - Cost effective - High sensitivity	Susceptible to outside environment	Enhance the stability through material improvement, structure design and encapsulation
	Piezoelectric	- Simple structure - Light and soft	- Susceptible to outside environment - High cost	Enhance the stability
	Electromagnetic	High output power	Rigid and bulky structure make a weak wearing comfort	Miniaturization
Temperature	Pyroelectric	Simple structure	- Slow response speed - High cost	Enhance the response speed through material modification
Humidity	Hygroelectric	- Simple structure - Light and soft	- Susceptible to outside environment - Limited choice of materials	Expand the scope of materials and enhance the stability
Molecular	Triboelectric	- Wide material chosen - High output voltage - Light and soft - Cost effective - High sensitivity - Various target markers detection	Susceptible to outside environment	Enhance the stability through material improvement, structure design and encapsulation

there are still some challenges that are described as follows.

5.1. Miniaturization

Most of the respiration monitoring devices are placed on the masks, bands or straps. To ensure comfort of the users, the devices should be fabricated as small as possible. Nowadays, some researchers make use of flexible materials to fabricate self-powered respiration sensors, thus improved the comfort of users (Pu et al., 2021). The self-powered sensors can get rid of the dependence of the external power supply, which has an advantage to further reduce the dimensions of the devices. Meanwhile, the rapid developed micro/nanofabrication technologies might provide a more sophisticated way to make an integrated and miniaturized system. In the future, a flexible and stretchable miniaturized self-powered respiration monitoring device is a promising wearable personalized equipment.

5.2. Stability

Physical and biochemical indexes of breath behavior including respiratory rhythm, respiratory intensity, acetone, breathing humidity and so on can reflect the health or respiratory disease of human body. If some devices were able to detect most of the above indexes in real time and simultaneously, the stability of the devices cannot be ignored. Optimizing the encapsule strategy of the system such as coating the device with thin layers of stretchable polymers may be in favor of its stability. At present, most of the respiration monitoring systems should be restricted to particular area to get reliable output signals (Dinh et al., 2020; Tang et al., 2019). The operating life and antijamming capability of respiration sensors play important roles in future development. Especially for real time and long-term detection, how to keep a stable sensing property of the self-powered system during the daily life is a huge challenge.

5.3. Output enhanced

The recent self-powered sensors or systems still faces the limitation of the power supplies. Although virous approaches such as piezoelectric, triboelectric, pyroelectric devices that can harvest energy from surrounding environment (Huang et al., 2016; Mahbub et al., 2017; Qi and McAlpine, 2010), the energy efficiency is not enough to match the power consumption of the whole respiration monitoring system. How to improve the outputs of the energy harvesting device to drive the system in real time will be a huge challenge. Meanwhile, the sensor data of the self-powered respiration monitoring system should be sent to the terminals like computer and mobile phone to deal with the data and provide the analysis of the respiratory status for the users. To ensure the wearing comfort of the device, wireless data transmission is essential. Then, the wireless transmission of detected signals means more power consumption of the devices. For example, the average power consumption is at the level of several to dozens of milliwatt, which is larger than outputs of most of miniaturized wearable energy harvesting devices.

5.4. Disease diagnosis

Researchers have developed considerable nanomaterial-based sensors to detect the diseases related to respiratory signals (Alkhouri et al., 2014; Broza and Haick, 2013; Tisch and Haick, 2014). However, there is a distance from accurate medical diagnosis. The further objective of the respiration monitoring system is to give pre-diagnostic result and professional recommendation for both consumers and doctors. What insufficient is that the recent self-powered respiration sensors cannot provide enough results about respiratory disease diagnosis. The key difficulty is the individual difference of the breath condition of each user will cause signal differences, which brings many challenges to make an accurate diagnosis of respiratory disease. One of the possible solutions is utilizing artificial intelligence to deal with the sensing signals, which has been widely used for disease diagnosis. On the other hand, the self-powered respiration monitoring systems toward modern medical diagnosis and health care need to be multi-functionalization. Commonly, making diagnosis of respiratory disease requires health information on many aspects, such as the volume of gas transferred, breathing frequency and volatile organic compounds in the exhalation. Recently, the rapid development and popularization of 5G bring us significant benefits to wireless sensor system in smart city, which means huge database for artificial intelligence and higher accuracy on respiratory illness. We can hopefully enjoy the convenience of digital communication consists of self-powered wireless sensors in the near future.

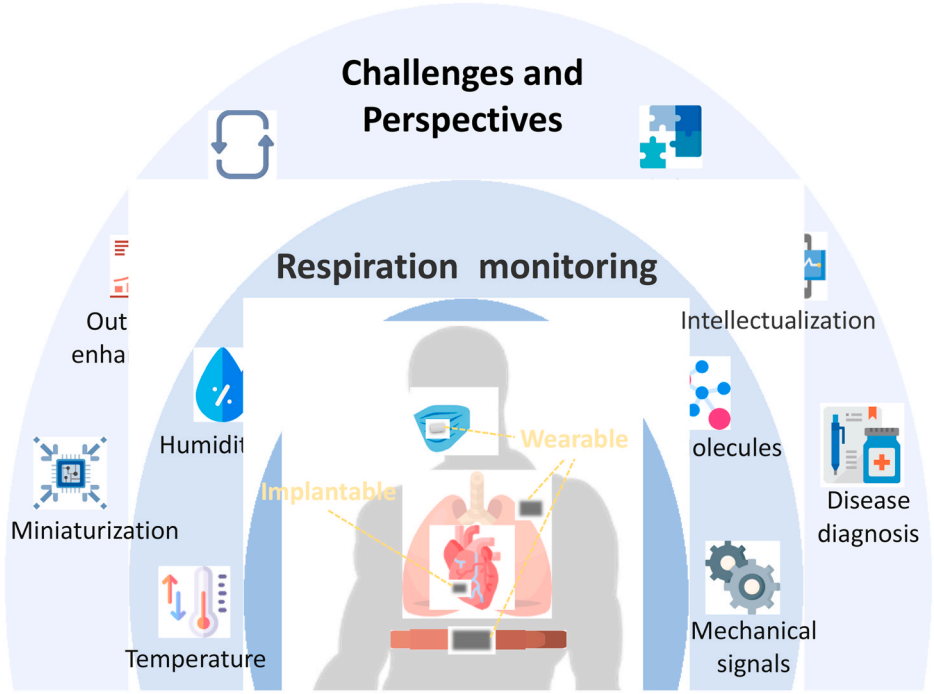

Fig. 6. Schematic illustration of conclusions and perspectives of self-powered respiration monitoring system. Designed by iconixar from Flaticon.

Declaration of competing interest

The authors declare that they have no known competing financial interests or personal relationships that could have appeared to influence the work reported in this paper.

Acknowledgement

This work was supported by the National Natural Science Foundation of China (T2125003, 61875015), Beijing Natural Science Foundation (JQ20038, 7204275), the Fundamental Research Funds for the Central Universities and the National Youth Talent Support Program.

References

Alam, M.M., Lee, S., Kim, M., Han, K.S., Cao, V.A., Nah, J., 2020. Ultra-flexible nanofiber-based multifunctional motion sensor. Nanomater. Energy 72, 104672.
Alkhouri, N., Cikach, F., Eng, K., Moses, J., Patel, N., Yan, C., Hanouneh, I., Grove, D., Lopez, R., Dweik, R., 2014. Analysis of breath volatile organic compounds as a noninvasive tool to diagnose nonalcoholic fatty liver disease in children. Eur. J. Gastroenterol. Hepatol. 26 (1), 82–87.
Alkhouri, N., Cikach, F., Eng, K., Patel, N., Yan, C., Brindle, A., Rome, E.S., Grove, D., Hanouneh, I.A., Lopez, R., Hazen, S.L., Dweik, R.A., 2013. Analysis of breath volatile organic compounds as a noninvasive tool to diagnose nonalcoholic fatty liver disease in obese children. Gastroenterology 144 (5), S947–S948.
Amann, A., Miekisch, W., Schubert, J., Buszewski, B., Ligor, T., Jezierski, T., Pleil, J., Risby, T., 2014. Analysis of exhaled breath for disease detection. Annu. Rev. Anal. Chem. 7, 455–482.
Bai, P., Zhu, G., Jing, Q.S., Yang, J., Chen, J., Su, Y.J., Ma, J.S., Zhang, G., Wang, Z.L., 2014. Membrane-based self-powered triboelectric sensors for pressure change detection and its uses in security surveillance and healthcare monitoring. Adv. Funct. Mater. 24 (37), 5807–5813.
Bai, Y., Jantunen, H., Juuti, J., 2018. Energy harvesting research: the road from single source to multisource. Adv. Mater. 30 (34), e1707271.
Barker, M., Hengst, M., Schmid, J., Buers, H.J., Mittermaier, B., Klemp, D., Koppmann, R., 2006. Volatile organic compounds in the exhaled breath of young patients with cystic fibrosis. Eur. Respir. J. 27 (5), 929–936.
Beeby, S.P., Torah, R.N., Tudor, M.J., Glynne-Jones, P., O'Donnell, T., Saha, C.R., Roy, S., 2007. A micro electromagnetic generator for vibration energy harvesting. J. Micromech. Microeng. 17 (7), 1257–1265.
Beeby, S.P., Tudor, M.J., White, N.M., 2006. Energy harvesting vibration sources for microsystems applications. Meas. Sci. Technol. 17 (12), R175–R195.
Bernal, W., Auzinger, G., Dhawan, A., Wendon, J., 2010. Acute liver failure. Lancet 376 (9736), 190–201.
Bodkhe, S., Noonan, C., Gosselin, F.P., Therriault, D., 2018. Coextrusion of multifunctional smart sensors. Adv. Eng. Mater. 20 (10), 1800206.
Boskovic, M.V., Sarajlic, M., Frantlovic, M., Smiljanic, M.M., Randjelovic, D.V., Zobenica, K.C., Radovic, D.V., 2020. Aluminum-based self-powered hyper-fast miniaturized sensor for breath humidity detection. Sensor. Actuator. B Chem. 321, 128635.
Broza, Y.Y., Haick, H., 2013. Nanomaterial-based sensors for detection of disease by volatile organic compounds. Nanomedicine 8 (5), 785–806.
Bruderer, T., Gaisl, T., Gaugg, M.T., Nowak, N., Streckenbach, B., Muller, S., Moeller, A., Kohler, M., Zenobi, R., 2019. On-line analysis of exhaled breath focus review. Chem. Rev. 119 (19), 10803–10828.
Buszewski, B., Kesy, M., Ligor, T., Amann, A., 2007. Human exhaled air analytics: biomarkers of diseases. Biomed. Chromatogr. 21 (6), 553–566.
Cao, R., Wang, J.N., Zhao, S.Y., Yang, W., Yuan, Z.Q., Yin, Y.Y., Du, X.Y., Li, N.W., Zhang, X.L., Li, X.Y., Wang, Z.L., Li, C.J., 2018. Self-powered nanofiber-based screen-print triboelectric sensors for respiratory monitoring. Nano Res 11 (7), 3771–3779.
Carpagnano, G.E., Foschino-Barbaro, M.P., Crocetta, C., Lacedonia, D., Saliani, V., Zoppo, L.D., Barnes, P.J., 2017. Validation of the exhaled breath temperature measure: reference values in healthy subjects. Chest 151 (4), 855–860.
Chan, L.W., Anahtar, M.N., Ong, T.H., Hern, K.E., Kunz, R.R., Bhatia, S.N., 2020. Engineering synthetic breath biomarkers for respiratory disease. Nat. Nanotechnol. 15 (9), 792–800.
Chao, S., Ouyang, H., Jiang, D., Fan, Y., Li, Z., 2020. Triboelectric nanogenerator based on degradable materials. EcoMat 3 (1), e12072.
Chen, G., Li, Y., Bick, M., Chen, J., 2020a. Smart textiles for electricity generation. Chem. Rev. 120 (8), 3668–3720.
Chen, G.R., Fang, Y.S., Zhao, X., Tat, T., Chen, J., 2021. Textiles for learning tactile interactions. Nat Electron 4 (3), 175–176.
Chen, S., Wu, N., Ma, L., Lin, S., Yuan, F., Xu, Z., Li, W., Wang, B., Zhou, J., 2018. Noncontact heartbeat and respiration monitoring based on a hollow microstructured self-powered pressure sensor. ACS Appl. Mater. Interfaces 10 (4), 3660–3667.
Chen, X., Li, X., Shao, J., An, N., Tian, H., Wang, C., Han, T., Wang, L., Lu, B., 2017a. High-performance piezoelectric nanogenerators with imprinted P(VDF-TrFE)/BaTiO3 nanocomposite micropillars for self-powered flexible sensors. Small 13 (23), 1604245.
Chen, X.L., Shao, J.Y., An, N.L., Li, X.M., Tian, H.M., Xu, C., Ding, Y.C., 2015. Self-powered flexible pressure sensors with vertically well-aligned piezoelectric nanowire arrays for monitoring vital signs. J. Mater. Chem. C 3 (45), 11806–11814.
Chen, X.P., Xie, X.K., Liu, Y.N., Zhao, C., Wen, M., Wen, Z., 2020b. Advances in healthcare electronics enabled by triboelectric nanogenerators. Adv. Funct. Mater. 30 (43), 2004673.
Chen, X.X., Song, Y., Su, Z.M., Chen, H.T., Cheng, X.L., Zhang, J.X., Han, M.D., Zhang, H. X., 2017b. Flexible fiber-based hybrid nanogenerator for biomechanical energy harvesting and physiological monitoring. Nanomater. Energy 38, 43–50.
Chen, Y.Q., Wang, L.R., Ko, W.H., 1990. A piezopolymer finger pulse and breathing wave sensor. Sensor Actuat a-Phys 23 (1–3), 879–882.
Cheng, Y., Lu, X., Chan, K.H., Wang, R.R., Cao, Z.R., Sun, J., Ho, G.W., 2017a. A stretchable fiber nanogenerator for versatile mechanical energy harvesting and

self-powered full-range personal healthcare monitoring. Nanomater. Energy 41, 511–518.
Cheng, Y.L., Wang, C.Y., Zhong, J.W., Lin, S.Z., Xiao, Y.J., Zhong, Q.Z., Jiang, H.L., Wu, N., Li, W.B., Chen, S.W., Wang, B., Zhang, Y.Y., Zhou, J., 2017b. Electrospun polyetherimide electret nonwoven for bi-functional smart face mask. Nanomater. Energy 34, 562–569.
Cho, M.Y., Kim, I.S., Kim, S.H., Park, C., Kim, N.Y., Kim, S.W., Kim, S., Oh, J.M., 2021. Unique noncontact monitoring of human respiration and sweat evaporation using a CsPb2Br5-based sensor. ACS Appl. Mater. Interfaces 13 (4), 5602–5613.
Chun, K.Y., Son, Y.J., Seo, S., Lee, H.J., Han, C.S., 2020. Nonlinearly frequency-adaptive, self-powered, proton-driven somatosensor inspired by a human mechanoreceptor. ACS Sens. 5 (3), 845–852.
Chung, H.U., Kim, B.H., Lee, J.Y., Lee, J., Xie, Z., Ibler, E.M., Lee, K., Banks, A., Jeong, J. Y., Kim, J., Ogle, C., Grande, D., Yu, Y., Jang, H., Assem, P., Ryu, D., Kwak, J.W., Namkoong, M., Park, J.B., Lee, Y., Kim, D.H., Ryu, A., Jeong, J., You, K., Ji, B., Liu, Z., Huo, Q., Feng, X., Deng, Y., Xu, Y., Jang, K.I., Kim, J., Zhang, Y., Ghaffari, R., Rand, C.M., Schau, M., Hamvas, A., Weese-Mayer, D.E., Huang, Y., Lee, S.M., Lee, C. H., Shanbhag, N.R., Paller, A.S., Xu, S., Rogers, J.A., 2019. Binodal, wireless epidermal electronic systems with in-sensor analytics for neonatal intensive care. Science 363 (6430), eaau0780.
Dagdeviren, C., Yang, B.D., Su, Y., Tran, P.L., Joe, P., Anderson, E., Xia, J., Doraiswamy, V., Dehdashti, B., Feng, X., Lu, B., Poston, R., Khalpey, Z., Ghaffari, R., Huang, Y., Slepian, M.J., Rogers, J.A., 2014. Conformal piezoelectric energy harvesting and storage from motions of the heart, lung, and diaphragm. Proc. Natl. Acad. Sci. U. S. A. 111 (5), 1927–1932.
de Gennaro, G., Dragonieri, S., Longobardi, F., Musti, M., Stallone, G., Trizio, L., Tutino, M., 2010. Chemical characterization of exhaled breath to differentiate between patients with malignant plueral mesothelioma from subjects with similar professional asbestos exposure. Anal. Bioanal. Chem. 398 (7–8), 3043–3050.
Ding, X., Cao, H., Zhang, X., Li, M., Liu, Y., 2018. Large scale triboelectric nanogenerator and self-powered flexible sensor for human sleep monitoring. Sensors 18 (6), 1713.
Dinh, T., Nguyen, T., Phan, H.P., Nguyen, N.T., Dao, D.V., Bell, J., 2020. Stretchable respiration sensors: advanced designs and multifunctional platforms for wearable physiological monitoring. Biosens. Bioelectron. 166, 112460.
Fan, F.R., Tang, W., Wang, Z.L., 2016. Flexible nanogenerators for energy harvesting and self-powered electronics. Adv. Mater. 28 (22), 4283–4305.
Fan, F.R., Tian, Z.Q., Wang, Z.L., 2012. Flexible triboelectric generator! Nanomater. Energy 1 (2), 328–334.
Fang, Z., Feng, J., Fu, X., Li, J., Hu, X., Xie, X., Yu, D., 2020. Humidity and pressure dual-responsive metal-water batteries enabled by three-in-one all-polymer cathodes for smart self-powered systems. ACS Appl. Mater. Interfaces 12 (21), 23853–23859.
Feng, H., Zhao, C., Tan, P., Liu, R., Chen, X., Li, Z., 2018. Nanogenerator for biomedical applications. Adv Healthc Mater 7 (10), e1701298.
Feng, J., Xiao, M., Hui, Z., Shen, D., Tian, Y., Hang, C., Duley, W.W., Zhou, N.Y., 2020. High-performance magnesium-carbon nanofiber hygroelectric generator based on interface-mediation-enhanced capacitive discharging effect. ACS Appl. Mater. Interfaces 12 (21), 24289–24297.
Fu, Y., He, H., Zhao, T., Dai, Y., Han, W., Ma, J., Xing, L., Zhang, Y., Xue, X., 2018. A self-powered breath analyzer based on PANI/PVDF piezo-gas-sensing arrays for potential diagnostics application. Nano-Micro Lett. 10 (4), 76.
Gandevia, S.C., McKenzie, D.K., 2008. Respiratory rate: the neglected vital sign. Med. J. Aust. 189 (9), 532.
Guo, H., Chen, J., Tian, L., Leng, Q., Xi, Y., Hu, C., 2014. Airflow-induced triboelectric nanogenerator as a self-powered sensor for detecting humidity and airflow rate. ACS Appl. Mater. Interfaces 6 (19), 17184–17189.
Haick, H., Broza, Y.Y., Mochalski, P., Ruzsanyi, V., Amann, A., 2014. Assessment, origin, and implementation of breath volatile cancer markers. Chem. Soc. Rev. 43 (5), 1423–1449.
Han, Y., Han, Y., Zhang, X., Li, L., Zhang, C., Liu, J., Lu, G., Yu, H.D., Huang, W., 2020. Fish gelatin based triboelectric nanogenerator for harvesting biomechanical energy and self-powered sensing of human physiological signals. ACS Appl. Mater. Interfaces 12 (14), 16442–16450.
Hashoul, D., Haick, H., 2019. Sensors for detecting pulmonary diseases from exhaled breath. Eur. Respir. Rev. 28 (152), 190011.
Hoffmann, T., Eilebrecht, B., Leonhardt, S., 2011. Respiratory monitoring system on the basis of capacitive textile force sensors. Ieee Sens J 11 (5), 1112–1119.
Huang, X., Wang, D., Yuan, Z., Xie, W., Wu, Y., Li, R., Zhao, Y., Luo, D., Cen, L., Chen, B., Wu, H., Xu, H., Sheng, X., Zhang, M., Zhao, L., Yin, L., 2018a. A fully biodegradable battery for self-powered transient implants. Small 14 (28), e1800994.
Huang, Y., Kershaw, S.V., Wang, Z., Pei, Z., Liu, J., Huang, Y., Li, H., Zhu, M., Rogach, A. L., Zhi, C., 2016. Highly integrated supercapacitor-sensor systems via material and geometry design. Small 12 (25), 3393–3399.
Huang, Y.X., Cheng, H.H., Yang, C., Zhang, P.P., Liao, Q.H., Yao, H.Z., Shi, G.Q., Qu, L.T., 2018b. Interface-mediated hygroelectric generator with an output voltage approaching 1.5 volts. Nat. Commun. 9 (1), 4166.
Jiang, D., Shi, B., Ouyang, H., Fan, Y., Wang, Z.L., Li, Z., 2020. Emerging implantable energy harvesters and self-powered implantable medical electronics. ACS Nano 14 (6), 6436–6448.
Jiang, W., Li, H., Liu, Z., Li, Z., Tian, J.J., Shi, B.J., Zou, Y., Ouyang, H., Zhao, C.C., Zhao, L.M., Sun, R., Zheng, H.R., Fan, Y.B., Wang, Z.L., Li, Z., 2018. Fully bioabsorbable natural-materials-based triboelectric nanogenerators. Adv. Mater. 30 (32), 1801895.
Kano, S., Yamamoto, A., Ishikawa, A., Fujii, M., 2019. Respiratory rate on exercise measured by nanoparticle-based humidity sensor. 41st Annual International Conference of the Ieee Engineering in Medicine and Biology Society (Embc) 2019, 3567–3570.
Khandelwal, G., Raj, N.P.M.J., Kim, S.J., 2020. Triboelectric nanogenerator for healthcare and biomedical applications. Nano Today 33, 100882.
Kim, I., Roh, H., Kim, D., 2019. Willow-like portable triboelectric respiration sensor based on polyethylenimine-assisted CO2 capture. Nanomater. Energy 65, 103990.
Lama, J., Yau, A., Chen, G., Sivakumar, A., Zhao, X., Chen, J., 2021. Textile triboelectric nanogenerators for self-powered biomonitoring. J. Mater. Chem. https://doi.org/10.1039/D1TA02518J.
Lee, J.P., Lee, J.W., Baik, J.M., 2018. The progress of PVDF as a functional material for triboelectric nanogenerators and self-powered sensors. Micromachines 9 (10), 532.
Li, J., Kang, L., Long, Y., Wei, H., Yu, Y.H., Wang, Y.H., Ferreira, C.A., Yao, G., Zhang, Z. Y., Carlos, C., German, L., Lan, X.L., Cai, W.B., Wang, X.D., 2018. Implanted battery-free direct-current micro-power supply from in vivo breath energy harvesting. Acs Appl Mater Inter 10 (49), 42030–42038.
Li, X.Q., Sun, Q., Kan, Y., Zhu, Y.A., Pang, Z.Y., Li, M.J., Jin, Y., 2021a. Self-powered humidity sensor based on polypyrrole/melamine aerogel for real-time humidity monitoring. Ieee Sens J 21 (3), 2604–2609.
Li, X.Q., Sun, Q., Kan, Y., Zhu, Y.N., Pang, Z.Y., Jin, Y., Li, M.J., Chronakis, I.S., 2020. Self-powered humidity sensor based on polypyrrole modified melamine aerogel. Mater. Lett. 277, 128281.
Li, Y., Zhang, M., Hu, X., Yu, L., Fan, X., Huang, C., Li, Y., 2021b. Graphdiyne-based flexible respiration sensors for monitoring human health. Nano Today 39, 101214.
Liang, Y., Zhao, F., Cheng, Z.H., Zhou, Q.H., Shao, H.B., Jiang, L., Qu, L.T., 2017. Self-powered wearable graphene fiber for information expression. Nanomater. Energy 32, 329–335.
Liao, J.W., Zou, Y., Jiang, D.J., Liu, Z.Z., Qu, X.C., Li, Z., Liu, R.P., Fan, Y.B., Shi, B.J., Li, Z., Zheng, L., 2020. Nestable arched triboelectric nanogenerator for large deflection biomechanical sensing and energy harvesting. Nanomater. Energy 69, 104417.
Lin, S.Z., Cheng, Y.L., Mo, X.W., Chen, S.W., Xu, Z.S., Zhou, B.P., Zhou, H., Hu, B., Zhou, J., 2019. Electrospun polytetrafluoroethylene nanofibrous membrane for high-performance self-powered sensors. Nanoscale Res Lett 14, 251.
Liu, Z., Li, H., Shi, B.J., Fan, Y.B., Wang, Z.L., Li, Z., 2019a. Wearable and implantable triboelectric nanogenerators. Adv. Funct. Mater. 29 (20), 1808820.
Liu, Z., Zhang, S., Jin, Y.M., Ouyang, H., Zou, Y., Wang, X.X., Xie, L.X., Li, Z., 2017. Flexible piezoelectric nanogenerator in wearable self-powered active sensor for respiration and healthcare monitoring. Semicond. Sci. Technol. 32 (6), 064004.
Liu, Z.X., Zhao, Z.Z., Zeng, X.W., Fu, X.L., Hu, Y., 2019b. Expandable microsphere-based triboelectric nanogenerators as ultrasensitive pressure sensors for respiratory and pulse monitoring. Nanomater. Energy 59, 295–301.
Lodge, R.A., Bhushan, B., 2007. Effect of physical wear and triboelectric interaction on surface charge as measured by Kelvin probe microscopy. J. Colloid Interface Sci. 310 (1), 321–330.
Logan, T.S., Taylor, R.K., 1930. Effect of water on triboelectric luminescence with mercury in glass. Science 72 (1856), 89–90.
Luo, R., Dai, J., Zhang, J., Li, Z., Accelerated skin wound healing by electrical stimulation. Adv Healthc Mater 10(16), 2100557.
Ma, Y., Zheng, Q., Liu, Y., Shi, B.J., Xue, X., Ji, W.P., Liu, Z., Jin, Y.M., Zou, Y., An, Z., Zhang, W., Wang, X.X., Jiang, W., Xu, Z.Y., Wang, Z.L., Li, Z., Zhang, H., 2016. Self-powered, one-stop, and multifunctional implantable triboelectric active sensor for real-time biomedical monitoring. Nano Lett. 16 (10), 6042–6051.
Mahbub, I., Oh, T., Shamsir, S., Islam, S.K., Pullano, S.A., Fiorillo, A.S., 2017. Design of a pyroelectric charge amplifier and a piezoelectric energy harvester for a novel non-invasive wearable and self-powered respiratory monitoring system. Ieee Reg 10 Humanit, 105–108.
Newnham, R.E., Skinner, D.P., Cross, L.E., 1978. Connectivity and piezoelectric-pyroelectric composites. Mater. Res. Bull. 13 (5), 525–536.
Ouyang, H., Jiang, D., Fan, Y., Wang, Z.L., Li, Z., 2021. Self-powered technology for next-generation biosensor. Sci. Bull. 66 (17), 1709–1712.
Paredi, P., Kharitonov, S.A., Barnes, P.J., 2000. Elevation of exhaled ethane concentration in asthma. Am J Resp Crit Care 162 (4), 1450–1454.
Paredi, P., Kharitonov, S.A., Barnes, P.J., 2002. Analysis of expired air for oxidation products. Am J Resp Crit Care 166 (12), S31–S37.
Park, K.I., Son, J.H., Hwang, G.T., Jeong, C.K., Ryu, J., Koo, M., Choi, I., Lee, S.H., Byun, M., Wang, Z.L., Lee, K.J., 2014. Highly-efficient, flexible piezoelectric PZT thin film nanogenerator on plastic substrates. Adv. Mater. 26 (16), 2514–2520.
Pasquel, F.J., Umpierrez, G.E., 2014. Hyperosmolar hyperglycemic state: a historic review of the clinical presentation, diagnosis, and treatment. Diabetes Care 37 (11), 3124–3131.
Pu, X.J., An, S.S., Tang, Q., Guo, H.Y., Hu, C.G., 2021. Wearable triboelectric sensors for biomedical monitoring and human-machine interface. Iscience 24 (1), 102027.
Qi, Y., McAlpine, M.C., 2010. Nanotechnology-enabled flexible and biocompatible energy harvesting. Energy Environ. Sci. 3 (9), 1275–1285.
Raj, N.P.M.J., Alluri, N.R., Vivekananthan, V., Chandrasekhar, A., Khandelwal, G., Kim, S.J., 2018. Sustainable yarn type-piezoelectric energy harvester as an eco-friendly, costeffective battery-free breath sensor. Appl. Energy 228, 1767–1776.
Rajabi-Abhari, A., Kim, J.N., Lee, J., Tabassian, R., Mahato, M., Youn, H.J., Lee, H., Oh, I. K., 2021. Diatom bio-silica and cellulose nanofibril for bio-triboelectric nanogenerators and self-powered breath monitoring masks. Acs Appl Mater Inter 13 (1), 219–232.
Rao Alluri, N., Vivekananthan, V., Chandrasekhar, A., Kim, S.J., 2018. Correction: adaptable piezoelectric hemispherical composite strips using a scalable groove technique for a self-powered muscle monitoring system. Nanoscale 10 (6), 3069.
Ray, P.P., 2018. A survey on Internet of Things architectures. J King Saud Univ-Com 30 (3), 291–319.
Reid, R.C., Mahbub, I., 2020. Wearable self-powered biosensors. Curr Opin Electroche 19, 55–62.

Roopa, G., Rajanna, K., Nayak, M.M., 2011. Non-Invasive human breath sensor. Ieee Sensor 1788–1791.
Roy, K., Ghosh, S.K., Sultana, A., Garain, S., Xie, M.Y., Bowen, C.R., Henkel, K., Schmeisser, D., Mandal, D., 2019. A self-powered wearable pressure sensor and pyroelectric breathing sensor based on GO interfaced PVDF nanofibers. Acs Appl Nano Mater 2 (4), 2013–2025.
Ryu, H., Kim, S.-W., 2021. Emerging pyroelectric nanogenerators to convert thermal energy into electrical energy. Small 17 (9), 1903469.
Sadri, B., Abete, A.M., Martinez, R.V., 2019. Simultaneous electrophysiological recording and self-powered biosignal monitoring using epidermal, nanotexturized, triboelectronic devices. Nanotechnology 30 (27), 274003.
Shahhaidar, E., Padasdao, B., Romine, R., Stickley, C., Boric-Lubecke, O., 2013. Piezoelectric and electromagnetic respiratory effort energy harvesters. Ieee Eng Med Bio 3443–3446.
Shahhaidar, E., Padasdao, B., Romine, R., Stickley, C., Lubecke, O.B., 2015. Electromagnetic respiratory effort harvester: human testing and metabolic cost analysis. Ieee J Biomed Health 19 (2), 399–405.
Shen, D.Z., Xiao, Y., Zou, G.S., Liu, L., Wu, A.P., Xiao, M., Feng, J.Y., Hui, Z., Duley, W. W., Zhou, Y.N., 2020. Exhaling-driven hydroelectric nanogenerators for stand-alone nonmechanical breath analyzing. Adv Mater Technol-Us 5 (1).
Sheng, H., Zhang, X., Liang, J., Shao, M., Xie, E., Yu, C., Lan, W., 2021. Recent advances of energy solutions for implantable bioelectronics. Adv Healthc Mater. https://doi.org/10.1002/adhm.202100199.
Shi, Q.F., He, T.Y.Y., Lee, C., 2019. More than energy harvesting - combining triboelectric nanogenerator and flexible electronics technology for enabling novel micro-/nano-systems. Nanomater. Energy 57, 851–871.
Shi, Y., Liu, R., He, L., Feng, H., Li, Y., Li, Z., 2020. Recent development of implantable and flexible nerve electrodes. Smart Materials in Medicine 1, 131–147.
Shin, D.M., Hong, S.W., Hwang, Y.H., 2020. Recent advances in organic piezoelectric biomaterials for energy and biomedical applications. Nanomaterials 10 (1), 123.
Shin, D.W., Barnes, M.D., Walsh, K., Dimov, D., Tian, P., Neves, A.I.S., Wright, C.D., Yu, S.M., Yoo, J.B., Russo, S., Craciun, M.F., 2018. A new facile route to flexible and semi-transparent electrodes based on water exfoliated graphene and their single-electrode triboelectric nanogenerator. Adv. Mater. 30 (39), 1892953.
Solga, S.F., 2014. Breath volatile organic compounds for the gut-fatty liver axis: promise, peril, and path forward. World J. Gastroenterol. 20 (27), 9017–9025.
Song, H.C., Kim, S.W., Kim, H.S., Lee, D.G., Kang, C.Y., Nahm, S., 2020. Piezoelectric energy harvesting design principles for materials and structures: material figure-of-merit and self-resonance tuning. Adv. Mater. 32 (51), e2002208.
Su, Y., Chen, G., Chen, C., Gong, Q., Xie, G., Yao, M., Tai, H., Jiang, Y., Chen, J., 2021a. Self-powered respiration monitoring enabled by a triboelectric nanogenerator. Adv. Mater. https://doi.org/10.1002/adma.202101262.
Su, Y., Li, W., Yuan, L., Chen, C., Pan, H., Xie, G., Conta, G., Ferrier, S., Zhao, X., Chen, G., Tai, H., Jiang, Y., Chen, J., 2021b. Piezoelectric fiber composites with polydopamine interfacial layer for self-powered wearable biomonitoring. Nanomater. Energy 89, 106321.
Su, Y., Wang, J., Wang, B., Yang, T., Yang, B., Xie, G., Zhou, Y., Zhang, S., Tai, H., Cai, Z., Chen, G., Jiang, Y., Chen, L.Q., Chen, J., 2020a. Alveolus-inspired active membrane sensors for self-powered wearable chemical sensing and breath analysis. ACS Nano 14 (5), 6067–6075.
Su, Y., Yang, T., Zhao, X., Cai, Z., Chen, G., Yao, M., Chen, K., Bick, M., Wang, J., Li, S., Xie, G., Tai, H., Du, X., Jiang, Y., Chen, J., 2020b. A wireless energy transmission enabled wearable active acetone biosensor for non-invasive prediabetes diagnosis. Nanomater. Energy 74, 104941.
Sultana, A., Alam, M.M., Middya, T.R., Mandal, D., 2018. A pyroelectric generator as a self-powered temperature sensor for sustainable thermal energy harvesting from waste heat and human body heat. Appl. Energy 221, 299–307.
Sun, J.G., Yang, T.N., Wang, C.Y., Chen, L.J., 2018. A flexible transparent one-structure tribo-piezo-pyroelectric hybrid energy generator based on bio-inspired silver nanowires network for biomechanical energy harvesting and physiological monitoring. Nanomater. Energy 48, 383–390.
Sun, T., Shen, L., Jiang, Y., Ma, J., Lv, F., Ma, H., Chen, D., Zhu, N., 2020. Wearable textile supercapacitors for self-powered enzyme-free smartsensors. ACS Appl. Mater. Interfaces 12 (19), 21779–21787.
Tai, H., Wang, S., Duan, Z., Jiang, Y., 2020. Evolution of breath analysis based on humidity and gas sensors: potential and challenges. Sensor. Actuator. B Chem. 318, 128104.
Tang, X., Wu, C.Y., Gan, L., Zhang, T., Zhou, T.T., Huang, J., Wang, H., Xie, C.S., Zeng, D. W., 2019. Multilevel microstructured flexible pressure sensors with ultrahigh sensitivity and ultrawide pressure range for versatile electronic skins. Small 15 (10), 1804559.
Tao, X., 2019. Study of fiber-based wearable energy systems. Acc. Chem. Res. 52 (2), 307–315.
Tat, T., Libanori, A., Au, C., Yau, A., Chen, J., 2021. Advances in triboelectric nanogenerators for biomedical sensing. Biosens. Bioelectron. 171, 112714.
Tisch, U., Haick, H., 2014. Chemical sensors for breath gas analysis: the latest developments at the Breath Analysis Summit 2013. J. Breath Res. 8 (2), 027103.
Tricoli, A., Nasiri, N., De, S.Y., 2017. Wearable and miniaturized sensor technologies for personalized and preventive medicine. Adv. Funct. Mater. 27 (15), 1605271.
van de Kant, K.D.G., van der Sande, L.J.T.M., Jobsis, Q., van Schayck, O.C.P., Dompeling, E., 2012. Clinical use of exhaled volatile organic compounds in pulmonary diseases: a systematic review. Respir. Res. 13, 117.
Vasandani, P., Gattu, B., Wu, J.M., Mao, Z.H., Jia, W.Y., Sun, M.G., 2017. Triboelectric nanogenerator using microdome-patterned PDMS as a wearable respiratory energy harvester. Adv Mater Technol-Us 2 (6), 1700014.
Wang, B., Liu, C., Xiao, Y.J., Zhong, J.W., Li, W.B., Cheng, Y.L., Hu, B., Huang, L., Zhou, J., 2017a. Ultrasensitive cellular fluorocarbon piezoelectret pressure sensor for self-powered human physiological monitoring. Nanomater. Energy 32, 42–49.
Wang, G.X., Pei, Z.B., Ye, C.H., 2019a. Inkjet-printing and performance investigation of self-powered flexible graphene oxide humidity sensors. J. Inorg. Mater. 34 (1), 114–120.
Wang, M., Zhang, J.H., Tang, Y.J., Li, J., Zhang, B.S., Liang, E.J., Mao, Y.C., Wang, X.D., 2018. Air-flow-driven triboelectric nanogenerators for self-powered real-time respiratory monitoring. ACS Nano 12 (6), 6156–6162.
Wang, S., Jiang, Y.D., Tai, H.L., Liu, B.H., Duan, Z.H., Yuan, Z., Pan, H., Xie, G.Z., Du, X. S., Su, Y.J., 2019b. An integrated flexible self-powered wearable respiration sensor. Nanomater. Energy 63, 103829.
Wang, S., Tai, H.L., Liu, B.H., Duan, Z.H., Yuan, Z., Pan, H., Su, Y.J., Xie, G.Z., Du, X.S., Jiang, Y.D., 2019c. A facile respiration-driven triboelectric nanogenerator for multifunctional respiratory monitoring. Nanomater. Energy 58, 312–321.
Wang, S., Wang, Z.L., Yang, Y., 2016. A one-structure-based hybridized nanogenerator for scavenging mechanical and thermal energies by triboelectric–piezoelectric–pyroelectric effects. Adv. Mater. 28 (15), 2881–2887.
Wang, S.H., Mu, X.J., Wang, X., Gu, A.Y., Wang, Z.L., Yang, Y., 2015a. Elasto-aerodynamics-driven triboelectric nanogenerator for scavenging air-flow energy. ACS Nano 9 (10), 9554–9563.
Wang, S.H., Xie, Y.N., Niu, S.M., Lin, L., Wang, Z.L., 2014. Freestanding triboelectric-layer-based nanogenerators for harvesting energy from a moving object or human motion in contact and non-contact modes. Adv. Mater. 26 (18), 2818–2824.
Wang, Z.L., 2012. Self-powered nanosensors and nanosystems. Adv. Mater. 24 (2), 280–285.
Wang, Z.L., 2017. On Maxwell's displacement current for energy and sensors: the origin of nanogenerators. Mater. Today 20 (2), 74–82.
Wang, Z.L., Chen, J., Lin, L., 2015b. Progress in triboelectric nanogenerators as a new energy technology and self-powered sensors. Energy Environ. Sci. 8 (8), 2250–2282.
Wang, Z.L., Jiang, T., Xu, L., 2017b. Toward the blue energy dream by triboelectric nanogenerator networks. Nanomater. Energy 39, 9–23.
Wang, Z.L., Wang, A.C., 2019. On the origin of contact-electrification. Mater. Today 30, 34–51.
Wen, D.L., Liu, X., Deng, H.T., Sun, D.H., Qian, H.Y., Brugger, J., Zhang, X.S., 2019. Printed silk-fibroin-based triboelectric nanogenerators for multi-functional wearable sensing. Nanomater. Energy 66, 104123.
Wen, Z., Chen, J., Yeh, M.H., Guo, H.Y., Li, Z.L., Fan, X., Zhang, T.J., Zhu, L.P., Wang, Z. L., 2015. Blow-driven triboelectric nanogenerator as an active alcohol breath analyzer. Nanomater. Energy 16, 38–46.
Wu, C., Kim, T.W., Park, J.H., An, H., Shao, J.J., Chen, X.Y., Wang, Z.L., 2017. Enhanced triboelectric nanogenerators based on MoS2 monolayer nanocomposites acting as electron-acceptor layers. ACS Nano 11 (8), 8356–8363.
Wu, H., Huang, Y.A., Xu, F., Duan, Y.Q., Yin, Z.P., 2016. Energy harvesters for wearable and stretchable electronics: from flexibility to stretchability. Adv. Mater. 28 (45), 9881–9919.
Xia, X.N., Liu, G.L., Chen, L., Li, W.L., Xi, Y., Shi, H.F., Hu, C.G., 2015. Foldable and portable triboelectric-electromagnetic generator for scavenging motion energy and as a sensitive gas flow sensor for detecting breath personality. Nanotechnology 26 (47), 475402.
Xiao, Y., Shen, D.Z., Zou, G.S., Wu, A.P., Liu, L., Duley, W.W., Zhou, Y.N., 2019. Self-powered, flexible and remote-controlled breath monitor based on TiO2 nanowire networks. Nanotechnology 30 (32), 325503.
Xie, K.Y., Wei, B.Q., 2014. Materials and structures for stretchable energy storage and conversion devices. Adv. Mater. 26 (22), 3592–3617.
Xu, K., Fujita, Y., Lu, Y., Honda, S., Shiomi, M., Arie, T., Akita, S., Takei, K., 2021a. A wearable body condition sensor system with wireless feedback alarm functions. Adv. Mater. 33 (18), 2008701.
Xu, Q., Fang, Y., Jing, Q., Hu, N., Lin, K., Pan, Y., Xu, L., Gao, H., Yuan, M., Chu, L., Ma, Y., Xie, Y., Chen, J., Wang, L., 2021b. A portable triboelectric spirometer for wireless pulmonary function monitoring. Biosens. Bioelectron. 187, 113329.
Xue, H., Yang, Q., Wang, D.Y., Luo, W.J., Wang, W.Q., Lin, M.S., Liang, D.L., Luo, Q.M., 2017. A wearable pyroelectric nanogenerator and self-powered breathing sensor. Nanomater. Energy 38, 147–154.
Xue, X.Y., Fu, Y.M., Wang, Q., Xing, L.L., Zhang, Y., 2016. Outputting olfactory bionic electric impulse by PANI/PTFE/PANI sandwich nanostructures and their application as flexible, smelling electronic skin. Adv. Funct. Mater. 26 (18), 3128–3138.
Yang, C., Huang, Y.X., Cheng, H.H., Jiang, L., Qu, L.T., 2019. Rollable, stretchable, and reconfigurable graphene hygroelectric generators. Adv. Mater. 31 (2), e1805705.
Yang, J., Chen, J., Su, Y.J., Jing, Q.S., Li, Z.L., Yi, F., Wen, X.N., Wang, Z.N., Wang, Z.L., 2015. Eardrum-inspired active sensors for self-powered cardiovascular system characterization and throat-attached anti-interference voice recognition. Adv. Mater. 27 (8), 1316–1326.
Yang, T., Pan, H., Tian, G., Zhang, B.B., Xiong, D., Gao, Y.Y., Yan, C., Chu, X., Chen, N.J., Zhong, S., Zhang, L., Deng, W.L., Yang, W.Q., 2020. Hierarchically structured PVDF/ZnO core-shell nanofibers for self-powered physiological monitoring electronics. Nanomater. Energy 72, 104706.
Ye, M.H., Cheng, H.H., Gao, J., Li, C.X., Qu, L.T., 2016. A respiration-detective graphene oxide/lithium battery. J. Mater. Chem. 4 (48), 19154–19159.
Zhang, B.S., Tang, Y.J., Dai, R.R., Wang, H.Y., Sun, X.P., Qin, C., Pan, Z.F., Liang, E.J., Mao, Y.C., 2019a. Breath-based human-machine interaction system using triboelectric nanogenerator. Nanomater. Energy 64, 103953.
Zhang, D.Z., Xu, Z.Y., Yang, Z.M., Song, X.S., 2020. High-performance flexible self-powered tin disulfide nanoflowers/reduced graphene oxide nanohybrid-based humidity sensor driven by triboelectric nanogenerator. Nanomater. Energy 67, 104251.

Zhang, S., Bick, M., Xiao, X., Chen, G., Nashalian, A., Chen, J., 2021a. Leveraging triboelectric nanogenerators for bioengineering. Matter 4 (3), 845–887.
Zhang, X., Ai, J., Zou, R., Su, B., 2021b. Compressible and stretchable magnetoelectric sensors based on liquid metals for highly sensitive, self-powered respiratory monitoring. ACS Appl. Mater. Interfaces 13 (13), 15727–15737.
Zhang, Z., Yan, Q., Liu, Z., Zhao, X., Wang, Z., Sun, J., Wang, Z.L., Wang, R., Li, L., 2021c. Flexible MXene composed triboelectric nanogenerator via facile vacuum-assistant filtration method for self-powered biomechanical sensing. Nanomater. Energy 88, 106257.
Zhang, Z., Zhang, J., Zhang, H., Wang, H., Hu, Z., Xuan, W., Dong, S., Luo, J., 2019b. A portable triboelectric nanogenerator for real-time respiration monitoring. Nanoscale Res Lett 14 (1), 354.
Zhao, F., Cheng, H.H., Zhang, Z.P., Jiang, L., Qu, L.T., 2015. Direct power generation from a graphene oxide film under moisture. Adv. Mater. 27 (29), 4351–4357.
Zhao, F., Wang, L., Zhao, Y., Qu, L., Dai, L., 2017. Graphene oxide nanoribbon assembly toward moisture-powered information storage. Adv. Mater. 29 (3), 1604972.
Zhao, H., Liu, L., Lin, X., Dai, J., Liu, S., Fei, T., Zhang, T., 2020. Proton-conductive gas sensor: a new way to realize highly selective ammonia detection for analysis of exhaled human breath. ACS Sens. 5 (2), 346–352.
Zhao, X., Askari, H., Chen, J., 2021. Nanogenerators for smart cities in the era of 5G and Internet of Things. Joule 5 (6), 1391–1431.
Zhao, Z.Z., Yan, C., Liu, Z.X., Fu, X.L., Peng, L.M., Hu, Y.F., Zheng, Z.J., 2016. Machine-Washable textile triboelectric nanogenerators for effective human respiratory monitoring through loom weaving of metallic yarns. Adv. Mater. 28 (46), 10267–10274.
Zheng, Q., Peng, M., Liu, Z., Li, S., Han, R., Ouyang, H., Fan, Y., Pan, C., Hu, W., Zhai, J., Li, Z., Wang, Z.L., 2021a. Dynamic real-time imaging of living cell traction force by piezo-phototronic light nano-antenna array. Science Advances 7 (22), eabe7738.
Zheng, Q., Shi, B.J., Fan, F.R., Wang, X.X., Yan, L., Yuan, W.W., Wang, S.H., Liu, H., Li, Z., Wang, Z.L., 2014. In vivo powering of pacemaker by breathing-driven implanted triboelectric nanogenerator. Adv. Mater. 26 (33), 5851–5856.
Zheng, Q., Tang, Q.Z., Wang, Z.L., Li, Z., 2021b. Self-powered cardiovascular electronic devices and systems. Nat. Rev. Cardiol. 18 (1), 7–21.
Zheng, Q., Zhang, H., Shi, B., Xue, X., Liu, Z., Jin, Y., Ma, Y., Zou, Y., Wang, X., An, Z., Tang, W., Zhang, W., Yang, F., Liu, Y., Lang, X., Xu, Z., Li, Z., Wang, Z.L., 2016. In vivo self-powered wireless cardiac monitoring via implantable triboelectric nanogenerator. ACS Nano 10 (7), 6510–6518.
Zhou, Y., Zhao, L.-D., 2017. Promising thermoelectric bulk materials with 2D structures. Adv. Mater. 29 (45), 1702676.
Zhou, Z., Chen, K., Li, X., Zhang, S., Wu, Y., Zhou, Y., Meng, K., Sun, C., He, Q., Fan, W., Fan, E., Lin, Z., Tan, X., Deng, W., Yang, J., Chen, J., 2020a. Sign-to-speech translation using machine-learning-assisted stretchable sensor arrays. Nat Electron 3 (9), 571–578.
Zhou, Z., Padgett, S., Cai, Z., Conta, G., Wu, Y., He, Q., Zhang, S., Sun, C., Liu, J., Fan, E., Meng, K., Lin, Z., Uy, C., Yang, J., Chen, J., 2020b. Single-layered ultra-soft washable smart textiles for all-around ballistocardiograph, respiration, and posture monitoring during sleep. Biosens. Bioelectron. 155, 112064.
Zhu, G., Peng, B., Chen, J., Jing, Q.S., Wang, Z.L., 2015. Triboelectric nanogenerators as a new energy technology: from fundamentals, devices, to applications. Nanomater. Energy 14, 126–138.
Zhu, M.M., Lou, M.N., Yu, J.Y., Li, Z.L., Ding, B., 2020. Energy autonomous hybrid electronic skin with multi-modal sensing capabilities. Nanomater. Energy 78, 105208.
Zi, Y., Guo, H., Wen, Z., Yeh, M.H., Hu, C., Wang, Z.L., 2016. Harvesting low-frequency (<5 Hz) irregular mechanical energy: a possible killer application of triboelectric nanogenerator. ACS Nano 10 (4), 4797–4805.
Zi, Y.L., Lin, L., Wang, J., Wang, S.H., Chen, J., Fan, X., Yang, P.K., Yi, F., Wang, Z.L., 2015. Triboelectric-pyroelectric-piezoelectric hybrid cell for high-efficiency energy-harvesting and self-powered sensing. Adv. Mater. 27 (14), 2340–2347.
Zou, Y., Bo, L., Li, Z., 2021. Recent progress in human body energy harvesting for smart bioelectronic system. Fundamental Research 1 (3), 364–382.
Zou, Y., Liao, J.W., Ouyang, H., Jiang, D.J., Zhao, C.C., Li, Z., Qu, X.C., Liu, Z., Fan, Y.B., Shi, B.J., Zheng, L., Li, Z., 2020. A flexible self-arched biosensor based on combination of piezoelectric and triboelectric effects. Appl Mater Today 20, 100699.